



Soft Ionics: Governing Physics and State of Technologies

Max Tepermeister¹, Nikola Bosnjak¹, Jinyue Dai¹, Xinyue Zhang², Samuel M. Kielar², Zhongtong Wang¹, Zhiting Tian¹, Jin Suntivich² and Meredith N. Silberstein^{1*}

¹Sibley School of Mechanical and Aerospace Engineering, Cornell University, Ithaca, NY, United States, ²Department of Materials Science and Engineering, Cornell University, Ithaca, NY, United States

OPEN ACCESS

Edited by:

Liheng Cai,
University of Virginia, United States

Reviewed by:

Shaoting Lin,
Massachusetts Institute of
Technology, United States
Michael Dickey,
North Carolina State University,
United States
Quan Chen,
Changchun Institute of Applied
Chemistry (CAS), China

*Correspondence:

Meredith N. Silberstein
meredith.silberstein@cornell.edu

Specialty section:

This article was submitted to
Soft Matter Physics,
a section of the journal
Frontiers in Physics

Received: 06 March 2022

Accepted: 29 April 2022

Published: 11 July 2022

Citation:

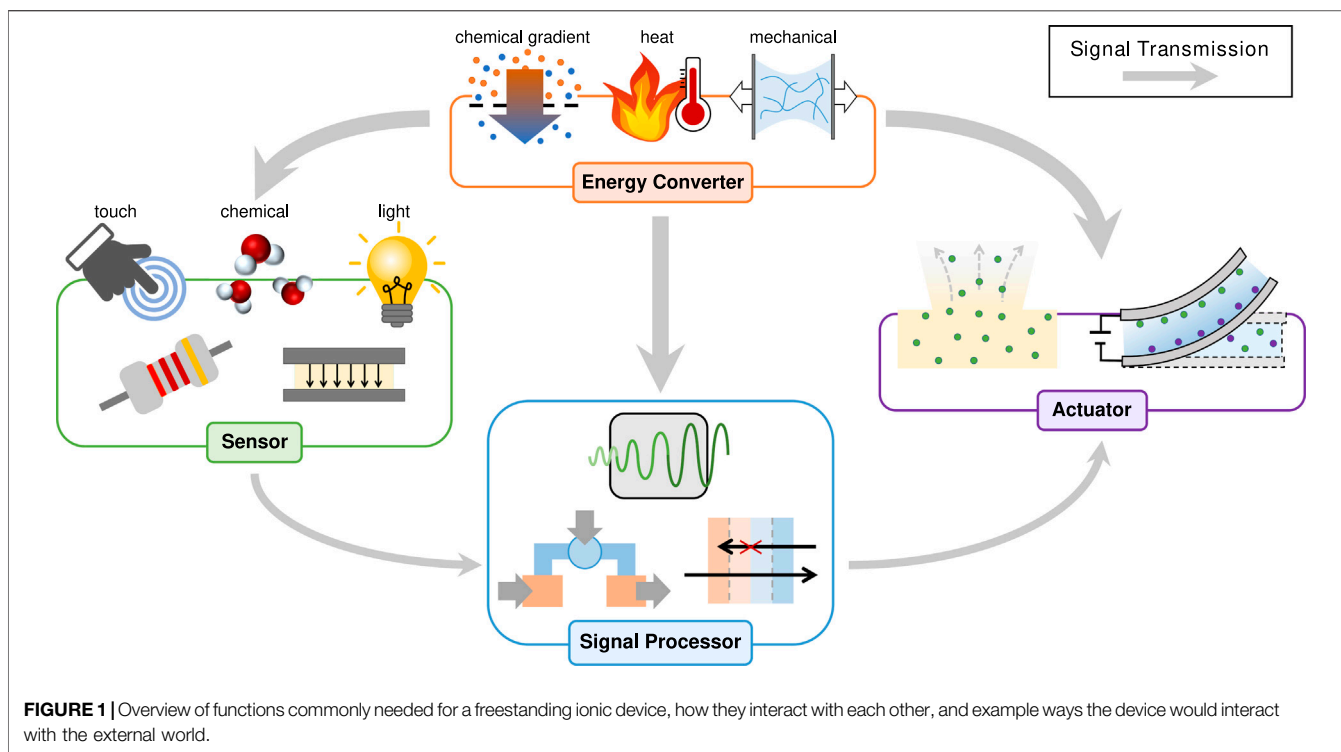
Tepermeister M, Bosnjak N, Dai J,
Zhang X, Kielar SM, Wang Z, Tian Z,
Suntivich J and Silberstein MN (2022)
Soft Ionics: Governing Physics and
State of Technologies.
Front. Phys. 10:890845.
doi: 10.3389/fphy.2022.890845

Soft ionic materials combine charged mobile species and tailored polymer structures in a manner that enables a wide array of functional devices. Traditional metal and silicon electronics are limited to two charge carriers: electrons and holes. Ionic devices hold the promise of using the wide range of chemical and molecular properties of mobile ions and polymer functional groups to enable flexible conductors, chemically specific sensors, bio-compatible interfaces, and deformable digital or analog signal processors. Stand alone ionic devices would need to have five key capabilities: signal transmission, energy conversion/harvesting, sensing, actuation, and signal processing. With the great promise of ionically-conducting materials and ionic devices, there are several fields working independently on pieces of the puzzle. These fields range from waste-water treatment research to soft robotics and bio-interface research. In this review, we first present the underlying physical principles that govern the behavior of soft ionic materials and devices. We then discuss the progress that has been made on each of the potential device components, bringing together findings from a range of research fields, and conclude with discussion of opportunities for future research.

Keywords: polyelectrolyte, ionomer, iontronics, soft robotics, electrochemistry, polymer, circuits

1 INTRODUCTION

Recent advances in soft ionic materials that incorporate mobile ions within flexible polymer matrices provide alternatives to traditional rigid inorganic materials, allowing devices to be deformable and have good performance [1]. Polymers have extensive tailorability due to the ease of changing their composition and sequence to tune physical/chemical properties. Furthermore, polymer-based materials often have advantages including low cost, ease of fabrication, biocompatibility, and operability in complex environments [2]. As the palette of multifunctional polymers continues to grow, researchers have begun imagining how they could be used to create an entirely new class of functional devices. The past 100 years have been marked by the dramatic development and proliferation of electronics. However, electrical conductors are generally limited to electrons (and sometimes holes) as their current carrying particles, and are typically rigid. Ionic conductors can take advantage of the wide array of ions. A single wire could carry many ion signals simultaneously, or interact directly with the ionic signalling found throughout nature. Ionic materials promise to usher in a new era of ionic devices that are more biocompatible, biointerfacing, flexible, and low-power than electronics. The developments necessary to realize fully ionic devices are occurring in many fields simultaneously, while the building blocks share similar fundamental science. We aim to bring an ionic device lens to the varied ways that potential ionic device components are discussed, described, conceptualized, and formalized across these different fields (Figure 1).



One essential function within a device is to move information from point A to point B. In ionic devices, this information takes the form of electric fields and chemical concentrations. In **Section 3.1**, we discuss the fundamental mechanisms for ion movement, and then talk about how researchers are improving the electrical, mechanical, and chemical properties of these ion signal carriers by tailoring the chemical composition, modifying the processing, and swelling the networks with different solvents and ions.

The next thing an ionic device must usually do is interact with its environment, bringing ion signals into and out of the device. These interactions with inputs and realizations of outputs take the form of sensors and actuators respectively. In **Section 3.2** we discuss the basic mechanisms of mechanical–ion coupling and then detail how researchers have used this coupling to create mechanical sensors and actuators. We then explore how tailored chemical functionalization is able to couple ionic polymers to other aspects of the environment like light, heat, and humidity.

After generating an ionic signal and transmitting it across the device, devices must process the incoming signal. In **Section 3.3** we discuss recent work creating ionic counterparts of electrical components like capacitors and transistors. We also discuss where the unique properties of polymers and ions enable device architectures not possible with traditional electronics, provide a categorization for diodes, and showcase state of the art ionic transistors.

Finally, ionic devices must follow the laws of thermodynamics, and thus moving information around and interacting with the outside world requires energy. There is simultaneously a deep literature on ionic power sources and little focus on powering ionic circuits. In **Section 3.4** we discuss energy storage and

conversion technologies we believe are promising for soft ionic devices.

We then conclude with our thoughts on opportunities for future device development and where our understanding of the underlying mechanisms remains both thin and critical.

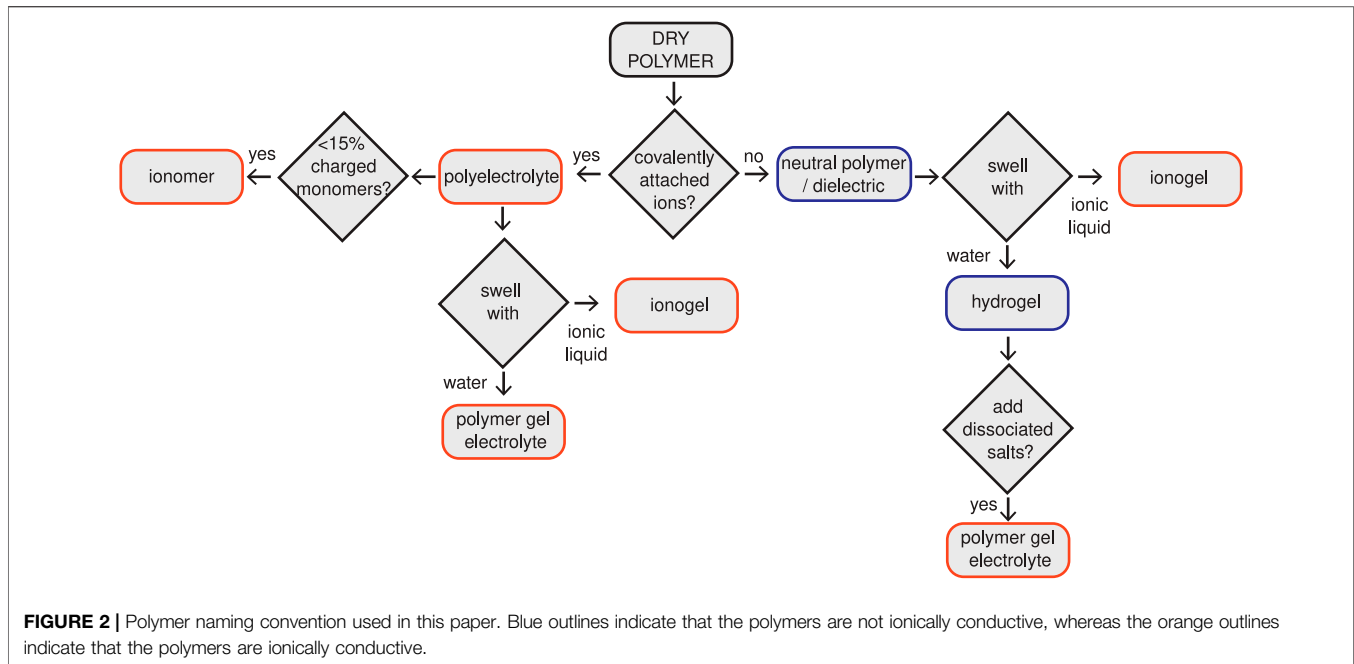
2 GOVERNING PHYSICS

2.1 Constituent Materials

Ionic devices are built from four main material types: electrical conductors, neutral gels, polyelectrolytes, and dielectric elastomers (see **Figure 2** for polymer naming convention). Each type is used for a variety of purposes, but shares a set of governing physics and common assumptions. For example, conductors can serve as both surface electrodes and internal conductive structures. This section details each material type, typical properties, and assumptions commonly made about each in the context of ionic devices.

2.1.1 Electrical Conductors

Electrical conductors are materials that allow electrons to flow freely inside them. They are able to accept and donate electrons of any energy level. The vast majority of conductors are metals. Some organic conjugated polymers like PEDOT:PSS (poly(3,4-ethylenedioxythiophene) polystyrene sulfonate) can also be conductors. Conductors generally follow Ohm's law, a linear relationship between the electric field across a conductor and the electric current that flows inside it. In physics this is generally written as in **Eq. 1**. Throughout this text, vectors are written with



a single underbar and second order tensors are written with a double underbar.

$$\underline{J} = \underline{\underline{\sigma}} \underline{E} \quad (1)$$

where \underline{E} is the local electric field, \underline{J} is the current density, and $\underline{\underline{\sigma}}$ is the conductivity tensor. In electrical engineering, components are typically lumped into discrete elements. As such, the local vector fields in physics are replaced with net currents and potentials. The electric field \underline{E} is integrated over the device length and becomes a voltage, V . The current density is integrated over the device area and becomes the total current, I . Finally, the conductivity is assumed isotropic, flattened to one dimension, and inverted to give a resistance, R . Taken together, these replacements give the engineering formulation of Ohm's law:

$$V = IR \quad (2)$$

When electrical conductors are used in ionic devices, their conductivity is typically orders of magnitude higher than the conductance of any other part of the system. This implies that the electric fields within conductors are smaller than in other parts of the system, and thus charge imbalances are only present at the boundaries. Therefore, they can carry large currents without large voltage drops. Electrical conductors in ionic devices are thus often assumed to contain no internal electric field and be at uniform voltage.

The most common use of conductors within ionic devices is as electrodes. These electrodes are often extremely thin films, and are thus assumed not to contribute to the mechanical properties of the device. Electrode design must still take into consideration the expected mechanical deformation of the device so as not to rupture or delaminate.

2.1.2 Neutral Gels

Neutral gels are crosslinked polymers that do not contain ionizable groups and are swollen in solvents. Most neutral gels used in ionic devices contain electrolytes with mobile ionic species. An electrolyte has mobile positive and negative ions. If swollen with water, they are generally referred to as hydrogels; the solvent content once swollen can exceed 99% by volume. If swollen with ionic liquids, they are referred to as ionogels. Ionogels tend to have greater stability and durability in air than hydrogels because they are not subject to water evaporation [3]. Neutral gels generally enable high mobility for a wide range of chemical species, which allows them to form the core of many ionic devices. They are to ions what electrical conductors are to electrons, and often act as ion carrying "wires". They additionally provide mechanical stability.

At smaller degrees of swelling, the porosity, connectivity, and chemical identity of the gel microstructure influence how easily mobile species move through it. They also determine how much and what type of solvent the gel can be swollen with [4]. Additionally, some gels have chemical functionality that allows them to change their properties in response to a stimulus. These stimuli can be light, chemical species, etc. as discussed in **Section 3.2** [5, 6]. The governing equations of gels can be broken up into mechanical, electrical, thermal, and diffusive parts, which can then be coupled together. For example, deformation can affect transport, and electric fields can induce stress.

There is a wealth of literature detailing the modelling of the mechanics of gels [7–9]. For most ionic devices, large-deformation isotropic incompressible elasticity captures the relevant features. This elasticity is typically given by the Neo-Hookean model for small to moderate deformation and the Gent or Arruda-Boyce models if stretches approaching failure are expected [10]. Expressions for the true stress under uniaxial

tension for the Neo-Hookean and Gent models are given by Eqs. 3 and 4 respectively.

$$\Sigma = G \left(\lambda^2 - \frac{1}{\lambda} \right) \quad (3)$$

$$\Sigma = G \frac{\lambda^2 - \lambda^{-1}}{1 - (\lambda^2 + 2/\lambda - 3)/I_m} \quad (4)$$

where Σ is the true stress in the direction of applied tension, λ is the stretch (ratio of final to initial length) in the direction of applied tension, G is the shear modulus that depends on the solvent content by $G \propto (V_{dry}/V_s)^{1/3}$ where V_s is the swollen gel volume and V_{dry} is the dry gel volume, and I_m is a material property that sets the stretch at which dramatic strain hardening will occur and will generally decrease with increasing solvent content. Most of the modelling complexity in gels for ionic devices comes from the interaction of their electric field, concentrations gradients, and mobile species. Electrochemical relations are covered in **Section 2.2**; mechano-electro-chemical-thermal coupling is discussed as technology relevant in **Section 3**.

Because gels provide the mechanical structure for most ionic devices, it is important that they can survive the stretching and deformation these devices undergo during operation. There has been significant work to improve the toughness and strength of gels. While covering this research in depth is out of scope of this paper, we direct readers to these papers on mechanical durability of hydrogels and ionogels [11–15].

2.1.3 Polyelectrolytes

The defining characteristic of polyelectrolytes is that they are polymers carrying ionizable moieties, which can dissociate in polar solvents, leaving charged groups covalently linked to polymer chains. These charged sites are balanced either by oppositely charged sites also fixed to polymer chains or by mobile charges. Polyelectrolytes with positive fixed charges are known as polycations, whereas polyelectrolytes with negative fixed charges are known as polyanions. Ionomers are a subclass of polyelectrolytes that have less than 15% of the monomers charged and for which these charged sites are typically phase segregated, forming a physical crosslink [16]. This fixed charge leads to one of the key behaviors of polyelectrolytes in ionic devices, which is referred to as Donnan exclusion: polycations tend to exclude mobile cations from their interior and polyanions tend to exclude mobile anions. Donnan exclusion, combined with the electrically insulating properties led to an alternative nomenclature for these materials when used as films: ion exchange membrane (IEM), cation exchange membrane (CEM), and anion exchange membrane (AEM) [17, 18].

Unlike gels, polyelectrolytes do not always contain additional solvent. The polyelectrolyte structure itself is sometimes sufficient for small ionic molecules to diffuse through it. Ionomers in particular tend to have reasonable ionic conductivity with relatively low solvent content because of the channels resulting from their phase segregated morphology [19], and therefore also tend to be stiffer and stronger than a hydrogel. Like gels, the mechanical properties of many polyelectrolytes can be well captured using the Neo-Hookean or Gent models (Eqs. 3 and 4). Many ionomers

and other lower solvent content polyelectrolytes are compressible and have viscoplasticity as a limit on device range of operation [20, 21].

2.1.4 Dielectric Elastomers

Dielectric elastomers are stretchable polymers that are neither ionically nor electrically conductive and thus lack long range charge mobility. They do have polymer bond dipoles that give rise to a dielectric constant (see **Section 2.2**) and so retain a linear internal electric field. In the context of ionic devices the main properties of interest are shear modulus, bulk modulus, and dielectric permittivity [22, 23].

2.2 Mobile Species Transport

The electrochemical performance of both polyelectrolytes and neutral gels in ionic devices is largely determined by the behavior of their mobile species. While modelling electric fields in materials, we assume that the speed of light is instantaneous compared to the rearrangement timescale of mobile charges. Therefore, we do not consider the propagation delay of electromagnetic fields, and thus use the electrostatic form of Maxwell's equations as given in Eqs. 5 and 6. **Equation 5** is the local form of Gauss's law and describes the relationship between the divergence of the electric field and the charge density. **Equation 6** states that the electric field is conservative.

$$\nabla \cdot \underline{E} = \frac{\rho}{\epsilon_0} \quad (5)$$

$$\nabla \times \underline{E} = 0 \quad (6)$$

where ρ is the charge density, ϵ_0 is the permittivity of free space, $\nabla \cdot$ is the divergence and $\nabla \times$ is the curl. **Equations 5** and **6** enable computation of the electric field everywhere given the charge distribution of the device under study. In a polyelectrolyte or gel there are three main forms of charges to be considered. First, there are the mobile charges; these take the form of ions like Na^+ or Cl^- , or mobile electrons. Second, there are the bound and balanced electrons and protons within the solvent or in the polymer chains. Third, there are charges bound within the polymer chains but uncompensated by bound opposite charges. We assume that bound charges quickly and locally rearrange themselves in response to external fields. This rearrangement occurs much faster (on the order of ns) than the ms timescale of many ionic devices, so we assume that these rearrangements happen instantly [24]. They do however affect the electric field within the material. The charge rearrangement gives rise to an additional material dielectric constant, ϵ_r , that represents how much polarization the quasi-neutral polymer chains and solvent undergo. An absolute permittivity, ϵ , is defined according to **Eq. 7**. Typical values for ϵ are approximately 3 for dielectric elastomers, 10 for ionogels, and 80 for hydrogels.

$$\epsilon = \epsilon_0 \epsilon_r \quad (7)$$

Plugging **Eq. 7** back into **Eq. 5** and defining ρ^* as the charge density of mobile charges and uncompensated polymer chain charges, we get a modified form of Gauss's law (**Eq. 8**)

$$\nabla \cdot \underline{E} = \frac{\rho^{*}}{\epsilon} \quad (8)$$

Finally, diffusive relations govern the flux of mobile species, including solvent, through the gel. See Narayan et al. for a detailed derivation [25]. The procedure at a high level is as follows: We define an electrochemical potential energy for each species that describes the energy cost associated with increasing the local concentration of that species. Systems tend to minimize their free energy, and thus tend to minimize their electrochemical potential. Separate species are often assumed to obey ideal solution mixing, where their interactions with other species are identical to their self-interactions. The gradient of this electrochemical potential is taken as a force driving the system to electrochemical equilibrium. An isotropic linear relationship is assumed between the gradient of the electrochemical potential and the flux of a particular mobile species. This process gives the Nernst-Planck equation shown in Eq. 9 where $\underline{J}^{(i)}$ is the flux, $z^{(i)}$ is the charge number, $C^{(i)}$ is the concentration, F is Faraday's constant, R is the universal gas constant, T is the temperature, and $u^{(i)}$ is the mobility of the i -th species.

$$\underline{J}^{(i)} = -u^{(i)}(RTVC^{(i)} + C^{(i)}z^{(i)}FVV) \quad (9)$$

Equation 9 describes the behavior of both neutral and charged species. For neutral species, the electric field does not contribute to their electrochemical potential because their charge number, $z^{(i)}$, is zero. For many gels and for the constituent solvent especially, ideal solution mixing is not a good assumption, since the solvent interacts differently with the polymer chains than it does with itself. Additionally, because the gel polymer matrix is able to exert mechanical forces it can exert a pressure on the solvent, which modifies the free energy. Consequently, the governing equations for the solvent are often described separately from the dilute mobile species.

The Nernst-Planck equation (Eq. 9) and Gauss's law (Eq. 8) lead to some fundamental device behaviors that are the main takeaways from this section. First, for mm scale devices, they ensure quasi-electrical neutrality throughout the vast majority of the device. Any electric dipole must either be limited to a small magnitude or a small length. The characteristic length scale over which electroneutrality is disobeyed is known as the Debye-Hückel length (λ_D).

$$\lambda_D = \sqrt{\frac{\epsilon RT}{2F^2 \sum_i (z^{(i)})^2 C_0^{(i)}}} \quad (10)$$

where $C_0^{(i)}$ is the initial concentration in mol m⁻³ of species i . λ_D decreases as concentration increases. For many polymer systems λ_D is on the order of 1–100 nm. These small length scales with large electric fields tend to occur at the polymer boundaries. In fact, the requirement to minimize free energy ensures that large changes in species concentration can only occur at similarly large discontinuities. This happens at boundaries with conductors, free space, other polymers, etc. Second, the current response of a

particular region of space to a given electric field strongly depends non-linearly on the concentration of mobile charged species in that region. This second feature is at the core of how many ionic devices amplify, change, and gate signals, and will be discussed in detail in Section 3.3. It is important to note that the equations discussed so far all rely on a statistical mechanical mean field assumption. That is, the space considered is large enough to allow the statistical average to dominate.

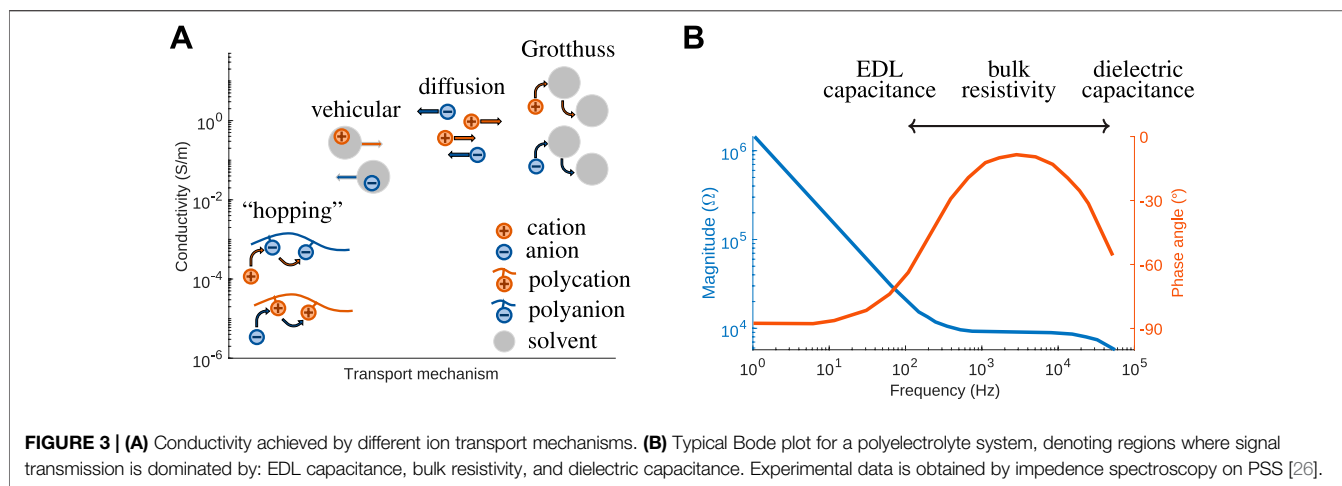
3 TECHNOLOGIES

In this section, we walk through the different ionic component functions that are commonly needed for independent soft ionic devices: signal transmission, sensing and actuating, signal transmuting (including memory), and energy/power sources.

3.1 Signal Transmission

Movement of mobile ions in response to an external stimuli allows for signal transmission across a soft ionic polymer. AC is a common way to achieve signal transmission through ionic conductors, especially when connected to an external electronic circuit. AC transmission is often preferable to DC because local ion concentration is maintained without concern for boundary conditions. DC transmission requires that ions are able to flow through an entire circuit without the impediment of non-ion-conducting materials and boundaries. Both transmission methods rely on the same ion transport mechanisms in the ionically conductive material (Figure 3A). The mechanisms shown in Figure 3A are the physics that underpin the magnitude of the ion mobility coefficient discussed in Eq. 9. This one coefficient includes combined contributions from each mechanism present in a given polymer.

One standard setup for AC ionic signal transmission is to place an ionically conductive material between two electrodes and apply a sinusoidal electric field. This causes the mobile ions to oscillate between the charged electrodes. Details of the transmission depend on frequency. At low frequencies, an electrical double layer (EDL) at the polymer electrode interface screens the charge by slowly charging and discharging in response to the alternating signal at the electrode surface (Figure 3B). The ionic current is out-of-phase with the input signal, observed as a phase angle approaches -90° , and the response of the material is governed by the interfacial properties, i.e., the capacitance of EDL. With an increase in frequency, the ionic signal becomes more in-phase with the applied signal, as the overall bulk properties become more dominant, leading to a resistor-like response, with the phase angle $\approx 0^\circ$. At high enough frequencies, very small time scales are insufficient for the EDL to fully charge/discharge. The rapid charge reorientation within the material leads to a response similar to that of a dielectric capacitor, and the phase angle approaches -90° again. The specific frequencies at which the device undergoes these transitions between in-phase and out-of-phase response are related to the Debye length, ionic mobility, and the distance between electrodes, and can be easily experimentally characterized by impedance spectroscopy so that it can be taken into account in device design.



Polyelectrolytes are candidates for ionic signal transmission because they can achieve relatively high conductivity. In hydrated CEMs, this high conductivity is primarily due to the Grotthuss mechanism—a transport mode involving rapid association and dissociation of protons to neighboring water molecules [27–29] (**Figure 3A**). The Grotthuss mechanism is also found in AEMs, where OH⁻ can be transported in a similar manner [30–32]. Another mechanism, found in hydrated polyelectrolytes, and also in hydrogels and ionogels, is *en masse* or vehicular transport. Here, charges are associated to solvent or water molecules, using them as “vehicles” for transport. Conductivity for this mode of transport is reported to be up to 1 S m⁻¹ [33]. In (nearly) dry IEMs, ions are transported by hopping along oppositely charged backbone sites. This results in a significantly lower conductivity. For example, experimental studies showed an increase in conductivity from ~10⁻⁵ S m⁻¹ to ~10¹ S m⁻¹ with an increase in relative humidity for Nafion membranes [33–36].

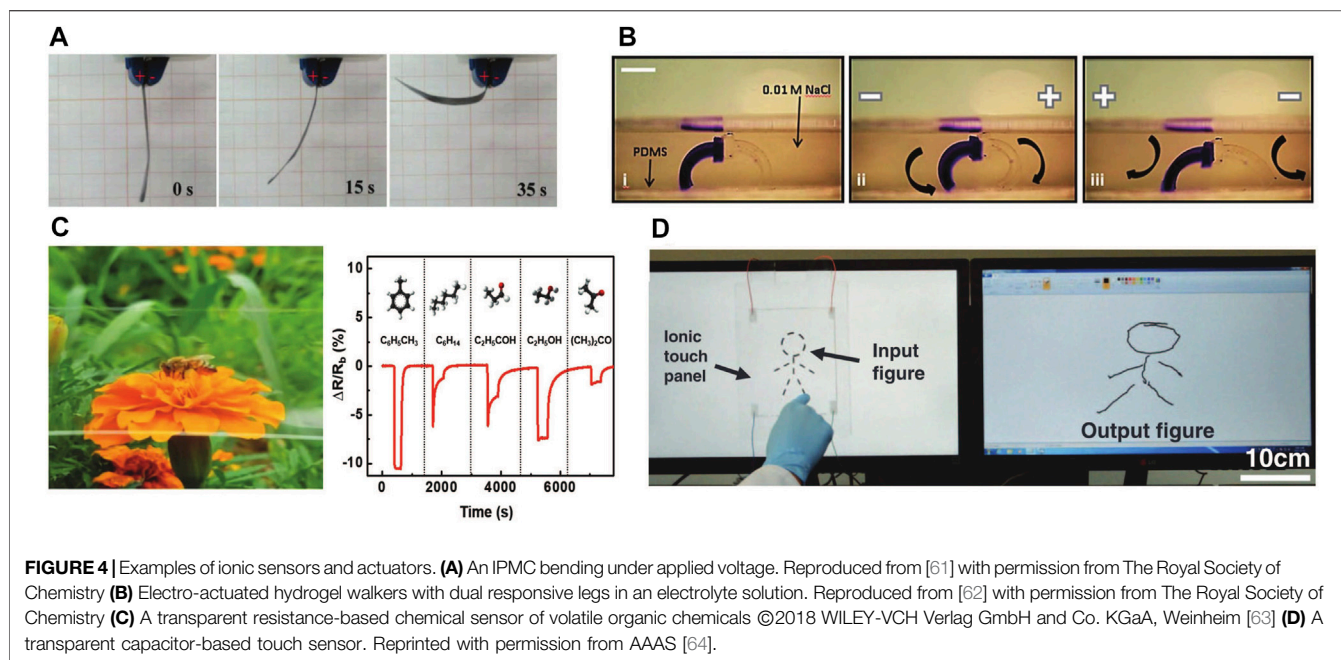
Commercial IEMs, such as Nafion and Neosepta, were initially designed for use in fuel cells; see Berezina et al. for a comprehensive list of commercial IEMs, along with their electrochemical features [37]. Their high conductivity and ion selective transport is also utilized in devices ranging from energy conversion and storage [38] to bioelectronics [39]. However, one of the main issues encountered in many such polyelectrolyte conductors is chemical and mechanical degradation due to repeated swelling and deswelling [40–42]. In addition, these materials are designed for applications where large deformation is unlikely to occur, and typically lack the necessary stretchability and toughness for use in deformable technologies. To overcome these issues, one recent approach in developing IEMs involves layer-by-layer fabrication of composite polyelectrolytes [43–45]. The layer-by-layer method enables nanoscale composites of otherwise challenging to combine materials.

Hydrogels and ionogels can also be good ionic conductors. Conductivity in these systems can be on the order of 1 S m⁻¹ [46], but generally decreases with increasing crosslink density [47], resulting in a tradeoff between mechanical and ionic transport properties. In one of the seminal publications on signal transmission employing hydrogels, Keplinger et al. reported on activation of a dielectric elastomer actuator (DEA) using

controlled ionic signal [1]. Flow of Na⁺ and Cl⁻ through a polyacrylamide hydrogel network was used to deliver charge and activate VHB (very high bond tape, 3M), a material widely used in DEA. The ionic signal was transmitted at frequencies exceeding 10 kHz and voltages above 10 kV, inducing rapid deformation of the DEA, sufficient for operating a loudspeaker. Building upon this seminal work, Yang et al. designed an ionic cable for signal transmission across significantly larger distance (45 cm), and at frequencies as high as 100 MHz [48]. Such performance was achieved by sandwiching a dielectric as an insulator between two parallel polyacrylamide conductors. The dielectric layer blocks charge transport between the parallel conductors, and each small segment of the cable behaves as a capacitor, charging and discharging in response to an AC signal. Chen et al. synthesized an ionogel capable of powering DEA in humidity ranging from 10% to 54% [49]. Such performance is achieved by infusing poly(acrylic acid) (PAA) with an ionic liquid. A similar concept of using ionogels to control DEA through ionic signals was also reported by Ming et al. [50]. More recently, Shi et al. reported ionic signal transmission in harsh environments by synthesizing an ionogel conductor using poly(ethyl acrylate) as the underlying polymer network [51]. This ionic conductor is capable of powering LEDs by ionic current at temperatures from -75°C to 75°C.

Self-healing is a desirable attribute for highly deformable ionic conductors, and in many cases arises naturally from the polymer structure. Cao et al. proposed an approach based on a polar polymer cross-linked by ion-dipole interactions and infused with ionic liquid [52]. Once healed, the material system proved capable of transmitting ionic current. More recently, Li et al. identified an elastomeric copolymer providing both self-healing properties and ionic conductivity, using it to power LEDs after healing [53]. Similarly, Zhao et al. demonstrated conductivity restoration upon self healing of PAA hydrogels with dissociated salt [54].

Ion selective transport, or ion exclusion, in charged polymeric backbones is another highly desirable feature which can be enhanced through layer-by-layer deposition. In contrast to filtering particles based on size, ion exclusion in polyelectrolytes typically arises due to electrostatic interaction



between the mobile ions and charged polymer backbone [55–57]. The multilayer structure, such as the one reported by Cheng et al. [58], allows for enhanced selectivity by excluding divalent ions. To complement the design of novel ion exchange materials and structures, development of computational tools for predicting this mechanism has gained significant attention in recent years [59, 60].

3.2 Sensing and Actuating

Over the last few decades, soft sensors and actuators have advanced substantially [65]. Here we focus on ionically conducting polymers only, excluding other electroactive polymers such as: intrinsically conducting (conjugated) polymers, dielectric elastomers, and liquid crystal elastomers, for which comprehensive reviews exist [66–73]. We divide the discussion below into swelling/deswelling driven actuators and sensors, resistive sensors, capacitive sensors, and ion release actuators.

3.2.1 Swelling Sensors and Actuators

Many soft actuators and sensors are based on swelling/deswelling processes. When driven by electric fields, these processes are typically related to flow of mobile ions that may also bring solvent with them, and add/subtract specific volume to/from the polymer. A second, less direct, pathway is that electrochemical reactions drive pH changes in the actuator/sensor environment that change the ionization state of the polymer and therefore its equilibrium swelling in solvent (osmotic pressure). These types of soft actuators and sensors are typically designed for either in-air or in-fluid operation, with different design considerations for each. In-air devices have flexible electrodes attached to their surfaces. In-fluid devices can have both, one, or no electrodes attached. We will start by discussing the both electrodes attached case—a device commonly known as an ionic polymer metal

composite (IPMC)—and then move on to the other cases, which operate only in a fluid environment.

IPMCs are bending mode actuators and sensors composed of a partially hydrated ionomer or polyelectrolyte-gel core, coated on each side with thin noble metal electrodes. The polymer is typically negatively charged, with mobile cation counter ions, but the reverse is possible. This bias towards polyanions is in large part due to their higher commercial availability and stability as compared to polycations [74]. As discovered simultaneously by Oguro et al. 1992, Shahinpoor et al. 1992, and Sadeghipour et al. 1992 [75–77], an applied voltage actuates bending (**Figure 4A**). A primary advantage of IPMCs, and ionic-based actuators more generally, is that they operate at relatively low voltages, typically in the range of 1V to 3V [66, 78]. The voltage drives cations to the cathode following the Nernst-Planck equations. These cations typically have a hydration shell that moves with them. The combined motion of the cations and solvent molecules causes expansion on the cathode side along with contraction on the anode side, that in concert lead to a bending motion. One downside of IPMC actuators is that they relax over time and eventually even bend in the opposite direction [78].

As sensors, IPMC respond to a bending type deformation, such as transverse tip deflection, since bending will drive motion of the ions and solvent. Sensing can be performed actively or passively through voltage, current, charge, impedance, or capacitance [78–82]. The passive approaches tend to be better for static deformation sensing and the active approaches tend to be better for dynamic deformation sensing. Each approach comes with trade-offs in terms of signal-to-noise, appropriate frequency range, environmental sensitivity, and device complexity. A primary deficiency of IPMCs as sensors is that the mechanical to electrical coupling is orders of magnitude weaker than the electrical to mechanical coupling [83].

Ionomer selection, ionomer processing, cation selection, and device geometry all critically influence IPMC performance. The most common ionomer used in IPMC is Nafion. Other common choices are Aciplex, Flemion, and PSS [61]. Each of these materials combines sufficiently high ion conductance and mechanical stiffness. The conductance, and to a lesser extent the mechanical properties, depend on the film processing and choice of cation. Ionogels and polymer electrolyte hydrogels can also be used as the polymer component of IPMC. The performance of hydrogel-based IPMC tend to suffer from drying out effects, but are promising from an ease of fabrication and bio-compatibility perspective [84]. Ionogel-based IPMC do not suffer from drying out and are less susceptible to back relaxation than ionomers in IPMC, but do tend to be less stiff and strong than ionomers [85–89]. Ion exchange of H^+ for Li^+ , Na^+ , K^+ , TMA^+ , etc. is also a common step in IPMC preparation since these other cations will have larger associated swelling strain [72]. The area of the electrode/polymer interface is also important because it sets the device capacitance. A wide range of approaches are used to create a large-area interaction between the ionomer and the noble-metal particulate electrode [74, 78, 90]. Finally, time scale and blocking force of the actuator are set by the mobility of the combined cations and hydration sphere and the thickness of the ionomer membrane. Relatively thin membranes are typically used ($\sim 200 \mu m$), keeping the timescale of response in the seconds or faster range and blocking forces in the mn range [72]. Device thickness can be increased to increase actuator blocking force, but it comes with a trade-off in actuator displacement and response time [78, 91, 92]. Blocking forces for IPMC are typically in the 1–100 mN regime [78, 93].

Extensive work over the last 2 decades has gone into modeling of IPMCs in both the actuator and sensor context [78, 83, 94, 95]; these models can be used to design devices such as grippers and assess their expected performance. Continuum modeling approaches work well for describing actuation but typically require some fitting parameters and still struggle with back relaxation [25, 83, 96–100]. Equivalent circuit modeling works well for IPMC sensors as this is a fast, low computational cost approach to modeling that facilitates integration of IPMC into more complex devices, including for self-sensing purposes [79, 101–104].

In solution, polyelectrolytes can be actuated through additional mechanisms to that described for IPMC above. These mechanisms arise because ions can move through the solution and into/out of the polymer. As nicely described by Glazer et al. [105], the two primary additional mechanisms of swelling driven actuation available in solution are: 1) pH changes resulting from electrolysis at the electrodes change the polyelectrolyte protonation and therefore its equilibrium dimensions in solution, 2) ions distribute unevenly across the gel/electrolyte interfaces because of Donnan exclusion and this local ionic strength variation drives local expansion or contraction changes by osmotic swelling (aka dynamic enrichment/depletion by [106]); this swelling will be different on the gel sides facing the anode and cathode. Relevance of the pH mechanism heavily depends on timescale of the device actuation,

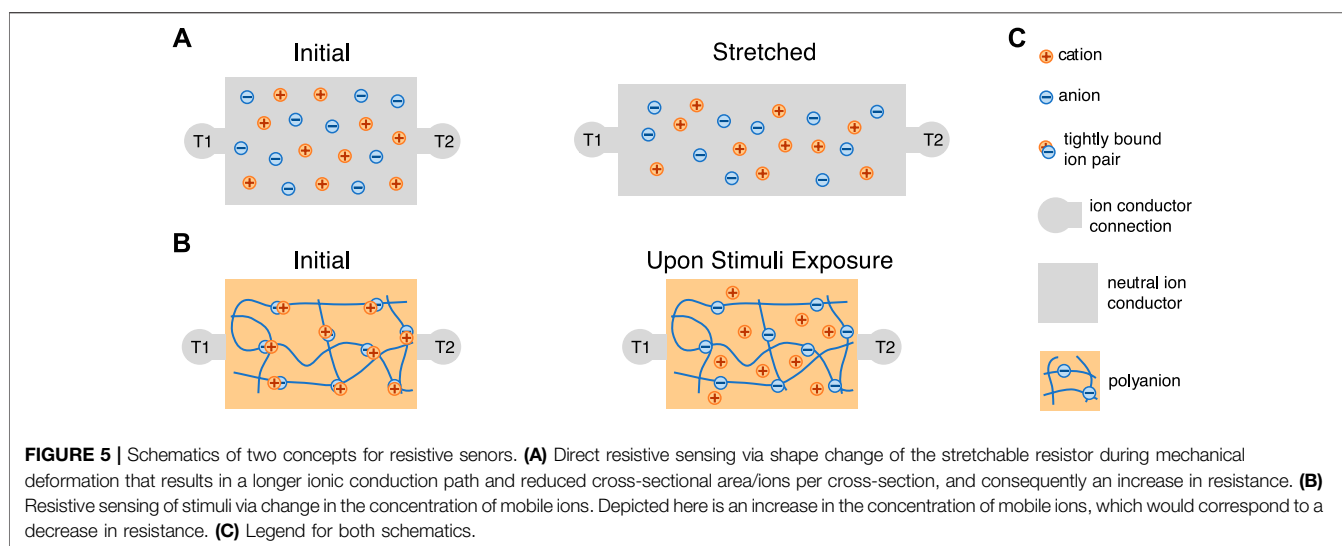
the size of the electrodes, and distance from the electrodes to the specimen: electrolysis produced ions must first be produced at significant concentration and then diffuse into the polymer. The dynamic enrichment mechanism is more widely relevant. Either mechanism can drive bending or overall volumetric contraction given appropriate specimen geometry. In many devices, both mechanisms contribute to actuation in a manner not simple to differentiate. The deformation of an acidic copolymer gel electrolyte in solution under an applied non-contact electric field was first observed by [107]. In 1992, Osada et. al. demonstrated bending of a polymer gel made of weakly crosslinked acidic copolymer immersed in a surfactant solution, when 20V was applied to electrodes 20 mm apart, that are parallel to each other and to the gel [108]. Much experimental [62, 109–116] and modeling [117–120] work has been done since then to develop these concepts into actuators, usually for soft robotics-type applications, and usually using bending mode deformation [62, 121–127]. One particularly exciting example is that of Morales et. al., who demonstrated a walker that works within an electrolyte solution (0.01 M NaCl) with one leg composed of an anionic gel and one leg composed of an cationic gel (**Figure 4B**) [62].

3.2.2 Resistive Sensors

Resistive sensing relies on a change in resistance in the device in response to the input that is being sensed. Within a sensor, this resistance change can result from geometric changes and/or ionic conductivity changes. Drilling down one step further, ionic conductivity changes can result from changes in either ion diffusivity or ion concentration.

Gels with mobile ionic components work directly as resistive strain sensors because their internal conduction path changes when uniaxial tension is applied. For a nearly incompressible material like a gel, the concentration of conductive ions will remain nearly constant under deformation, and therefore the conductance of the material will remain nearly constant as well. The conductive path length however, will increase by the tensile stretch λ , and the cross-sectional area will decrease by a factor of $1/\lambda$ (**Figure 5A**): the resistance therefore increases by a factor of λ^2 . For example, Cao et. al. synthesized a transparent, mechanically robust, and highly stable ionogel sensor using the poly(ethyl acrylate)-based elastomers and ionic liquids. The ionic liquid anions interact with the poly(ethyl acrylate) matrix via hydrogen bonding and increase the compatibility [128]. Much of the design concerns for these resistive strain sensors centers around enabling large reversible strain (e.g., by using a double network with dynamic and covalent bonds) and preventing loss of fluid from the gel (e.g., by using glycerol instead of water as the solvent) [129–133].

Ion concentration changes that result in resistance changes have been used to sense environmental humidity and have potential to sense light (**Figure 5B**). For many polyelectrolytes, ion dissociation commonly happens upon water absorption, making them natural humidity sensors [134–137]. For example, Yang et. al. demonstrated sulfonic acid doped poly(propargyl alcohol) as a humidity sensor: the presence of water facilitates the ionization of sulfonic acid as well as increases



the ion mobility. Thus the conductivity of the material increases as a function of the water vapor content [134]. Light has also recently been demonstrated as a method of modulating the ionic conductivity of polymer electrolytes, paving the way for these materials to be used as light sensors. This conductivity change in response to particular wavelengths was achieved by incorporating molecules that have photoswitchable binding of ions. Nie et. al. designed a copolymer with imidazolium-containing diarylethene (DAE) groups that bind to divalent nickel cations [138]. The DAE group is driven to a weaker metal binding ring open state by ultraviolet (UV) light and reverted to a stronger metal binding ring closed state by visible light. UV light therefore results in metal cations that move more freely through the material and overall a higher ionic conductivity material.

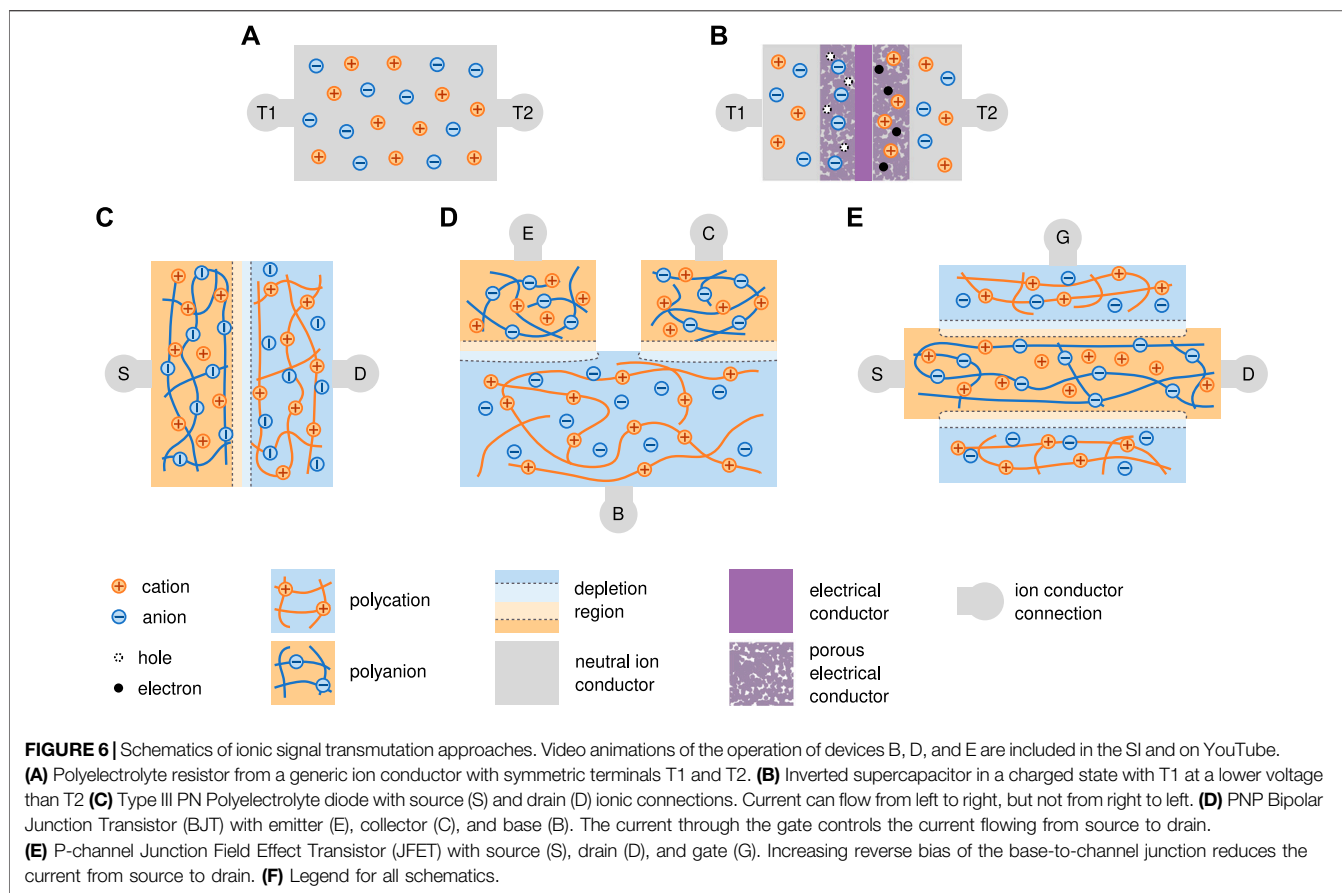
Finally, ionic mobility changes can be used for resistive sensors [63, 139, 140]. For example, Jin et. al. reported an ionic chemiresistor skin which can detect volatile organic compounds (VOCs). The core of the device is a highly stretchable ionogel film made of thermoplastic polyurethane matrix infused with ionic liquids. The sensor changes resistance when exposed to volatile organic compounds (VOCs) (Figure 4C). The ionic liquid viscosity decreases as the VOC concentration increases, and the viscosity decrease in turn increases ionic liquid diffusivity [63]. Similarly, a thermoplastic polyurethane-based ionogel was shown to detect temperature through temperature-dependent ionic mobility changes within the ionogel [140].

3.2.3 Capacitive Sensors

Changes in capacitance can be used for a variety of deformable sensor applications including stretch, touch, temperature, and humidity. Sun et. al. in 2014 introduced a configuration of two polymer electrolyte hydrogels sandwiching a soft dielectric for capacitive sensing [141]. The ionic hydrogels act as stretchable conductors, enabling measurement of changes in capacitance of

the dielectric elastomer resulting from deformation (shape changes). The authors were able to demonstrate reversible sensing of uniaxial tensile deformation, equibiaxial deformation, finger bending, and pressure sensing under touch. Lai et. al. was able to perform capacitive stretch sensing using a similar configuration, but with ionogels in place of polymer electrolyte hydrogels, leading to greater stability in air [131]. Kim et. al. utilized a bilayer of ionogels with opposite fixed charges and ionic liquid counterions, coated with carbon nanotube electrodes on opposite sides, to form a sensor that changes capacitance under in-plane tensile deformation. This capacitance change arises primarily across the interface of the two ionogels [142]. Kim et. al. took a distinct approach to achieve touch sensing using a polyelectrolyte hydrogel: they applied uniform voltage across a strip of the hydrogel that the touch disturbed (acting as a capacitor to a ground point), thereby driving an ionic current that could be measured (Figure 4D) [64]. Sawar et. al. took a third tact in using polymer gel electrolytes for sensing touch independent of sensor deformation. They created arrays of parallel architected polymer gel electrolytes separated by a dielectric layer. When a voltage is applied across the two polymer gel electrolyte electrodes, there is a projected electric field that interacts capacitively with a finger as it approaches. The finger location is determined by sweeping the sensor array [143]. Subsequent papers have extended these three sensing concepts in terms of material formulation and sensor geometry [131, 144–146].

Beyond these essentially mechanical sensors, IPMCs can also be made into capacitive-type humidity sensors [147, 148]. For example, Esmaeli et. al. built a IPMC-based humidity sensor based on Cr/Au or Ti/Au electrodes sandwiching a Nafion sheet. The dielectric constant of the IPMC changes when water molecules occupy the nano-channels inside Nafion, resulting in higher capacitance [147, 149]. Recently, Wang et. al. demonstrated that changes in the diffuse layer capacitance of



ion-conductor interfaces can be used to sense temperature [150]. They made a sandwich of hydrogel, dielectric elastomer, and a sensing electrode. As temperature increases, the Debye length increases, which lengthens the diffuse layer of the electrode double layer. This decreases the capacitance, which increases the voltage across the interface. The dielectric stops potential faradaic electrode reactions.

3.2.4 Ion Release Actuators

Ionic devices open the door to sensing and releasing biological signals, a feature highly utilized in many bioelectronic technologies, including controlled substance delivery actuators and neural recording sensors. In therapeutics, ion selectivity of PSS to conduct protons has been employed by [151] for targeted delivery of H^+ in response to an electric signal, while blocking the transport of Cl^- . Sjöström et al and Gabriëlsson et al. both demonstrated different PSS-based actuators capable of releasing the neurotransmitter acetylcholine. Sjöström et al. focused on miniaturization and speed, achieving release times on the order of ms, while Gabriëlsson achieved large continuous currents of neurotransmitter with longer time scales [152, 153]. There are also ion actuators known as organic electronic ion pumps. These use the oxidation of conjugated polymers (usually PEDOT:PSS) to drive the continuous migration of an ion from a source reservoir to a target reservoir [154,

155]. Lastly, while largely outside the scope of this review, there has been significant work using polyelectrolytes and hydrogels in electrical biointerfaces and bioelectronics that read and influence the electrical and ion environment of the body [156–158].

3.3 Transmuting the Signals

In electrical circuits, the basic linear elements are resistors, capacitors, and inductors. In addition to these linear elements, analog circuits often take advantage of nonlinear elements. The most common of these are the transistor and the diode. Memory could also be realized through nonlinear history-dependent resistors known as memristors [159–164], but to the authors' knowledge polymer or gel ionic memristors do not yet exist. Almost any analog circuit can be produced by a combination of these five elements. There has been significant work in the literature to create these elements using ions instead of electrons. The simplest of the above is the ionic resistor. This is an element that has a linear relationship between the electrochemical potential difference between two places and the ion current that flows between those two places. As discussed in prior sections (and Eq. 9), almost all ionically conducting polymers can act as a resistor (Figure 6A). Thus, we focus in the following sections on the other circuit elements (Figure 6, Supplementary Videos S1–S4).

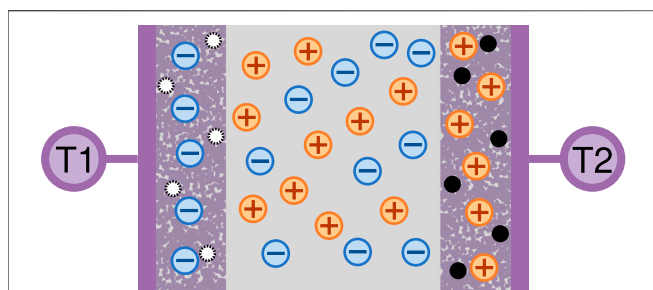


FIGURE 7 | The structure of a traditional electronic supercapacitor. Shown in a charged state with electrical terminal T1 at higher voltage and terminal T2 at lower voltage.

3.3.1 Capacitor

The second circuit element that has been recreated with ionics is the capacitor. Capacitors store energy in the form of electric fields. Generally they have a linear relationship between the stored charge and the voltage across them. One way to make an ionic capacitor is to sandwich a dielectric elastomer between two polymer electrolytes. Mobile ions in the electrolytes can then build up on opposite sides of the separating membrane and store energy in the resulting electric field. This is analogous to thin film solid state electrical capacitors. These devices tend to have low specific capacitances that are limited by the thickness of the separation layer but possess fast switching and charging times. They are also generally symmetric and thus can be charged in both polarities. Yang et al. created a capacitor of this type with two hydrogels separated by half a mm of VHB. Their device had an area of 2 cm^2 and a capacitance of 850 pF . This closely matches the theoretical parallel plate capacitance of 840 pF [48].

Ionic capacitors can also be made by inverting the structure of an electrolytic or super capacitor (Figure 7). In this setup, two electrolytes are separated by a thin electrically-conducting film. As the capacitor charges, ions build up on the two conductor faces. This build up induces a rearrangement of the charge inside the conductor, which leads to the formation of two double layers of charge, one at either side of the conductor (Figure 6B, Supplementary Video S1). The capacitance of these devices scales with the surface area of the ion-conductor interface. The larger this interface, the more ions can be stored at it for a given voltage. Janson et al. achieved a high specific capacitance by using PEDOT:PSS as the interface between a carbon conductor [165]. The size of this interface was about 4 mm^2 . The PEDOT:PSS is both an ionic conductor and an electrical conductor, and thus allows a very large number of ions to accumulate in its microstructure. As the device charges, electrons pass from one PSS interface to the other. This movement of charge changes the doping level in the PEDOT:PSS, oxidizing one side of the capacitor and reducing the other side. They reported a volumetric capacitance of 14.5 F cm^{-3} which is at least six orders of magnitude larger than the basic parallel plate capacitor. However, unlike the parallel capacitor, the PEDOT:PSS electrodes were limited to about 1 V before redox reactions like water splitting grew to dominate the charge transfer. The time constant of the capacitor charging was about 250 ms . Martin et al.

took a similar approach with different materials, making an inside out capacitor from reduced graphene oxide and a central PDMS ion barrier. Similar to Jansen et al., most of the volume of the device had both high ionic and electrical conductivity, while a small barrier region was only electrically conductive. This maximized the surface area available to create an ion double layer. They reported a volumetric capacitance of 4.31 F cm^{-3} with a time constant of approximately 5 s [167].

3.3.2 Diodes

Diodes are key nonlinear circuit elements. A polycation, with mobile counter anions, behaves similarly to an n-doped semiconductor, which has mobile negatively charged electrons. A polyanion, with mobile counter cations, behaves similarly to a p-doped semiconductor. When a polycation and polyanion are touched to each other, they form a bipolar membrane, which is a junction that behaves like a diode (Figure 6C, Supplementary Video S2). The specifics of how these devices function depends on the chemical identity of the mobile carriers in each polymer, as well as the mode of transport dominant in each polymer. Three diode classes are described below. To facilitate this description, we define some terminology and conventions. Device voltage is voltage at the mobile cation side minus voltage at the mobile anion side. For type II devices, device voltage is defined using with the initial locations of the non-interacting ion pair. Positive junction current is when positive charges flow from the mobile cation side to the mobile anion side or negative charges flow in the reverse direction. Open circuit voltage (OCV) is the device voltage when no current is flowing and the system is in electrochemical equilibrium. Applying voltages more positive than the open circuit voltage is called forward biasing; the converse is reverse biasing. Minority carriers are ions with the same charge and in the same region as fixed polyelectrolyte charges [167–169].

Type I diode: Annihilating ions with significant Donnan exclusion. This diode type is commonly created when bipolar membranes are placed between aqueous acid and base solutions. The membranes typically have high density of fixed charges and are selective to H^+ and OH^- . Under forward bias, H^+ and OH^- migrate toward the junction and combine to form water, which then diffuses away from the junction (similar to electron/hole annihilation in a traditional semiconductor PN junction). Under reverse bias, the mobile ions migrate away from the junction, leaving a region without charge carriers. This creates a large electric field that opposes the applied voltage and thus very little current flows in the device. If the reverse bias junction electric field is large enough, and there is a neutral species present in the junction made from the mobile ions (like H_2O), then this field can rip that neutral species apart into separate mobile charges and current will flow. This reverse bias breakdown can be intentionally used or suppressed, as discussed later.

Type II diode: Annihilating ions without significant Donnan exclusion. These diodes can be made from a hydrogel polyelectrolyte or a neutral gel, which does not exclude neutral salts. The rectification direction depends on the relative concentration of ionic charge carriers in baths bordering either side of the gel. Under forward bias, migration of the non-

annihilating counterions dominates. Under reverse bias, the current is lower because chemical recombination of the annihilating ions creates a region of neutral species right at the bath/polymer junction that is higher in resistance than the bulk polymer. If the gel is neutral, this device is called an electrolytic diode.

Type III diode: Non-annihilating ions with Donnan exclusion. This describes junctions between most polyelectrolytes. Under forward bias, the concentration of mobile carriers increases until it is sufficient to drive minority carriers into the opposing region. Therefore, forward bias current must be carried by minority carriers. Reverse operation is similar to type I, but if non-hydrogel polyelectrolytes are used, can sustain larger reverse voltages without breakdown.

With these categories in mind, there are four main metrics used to evaluate the performance of an ionic diode: rectification ratio, forward bias current, (reverse) breakdown voltage, and switching time. Rectification ratio is the ratio of the current flowing through a diode under forward bias to the current in reverse bias. Note that for the small voltages often used for polyelectrolyte diodes, it is important whether the voltages used to bias the diode are centered around the open circuit voltage, or instead around 0 V. The current under forward bias is determined by the applied voltage and conductivity at the transition from an exponential growth to an ohmic I-V curve with increasing forward bias voltage. The breakdown voltage refers to the voltage where the current begins to increase dramatically under reverse bias of the junction. Finally, the switching time refers to how long the diode takes to reach a steady state current after a transition from reverse to forward bias or vice versa.

The simplest polymer diode is a type II electrolytic diode with only one material layer that separates baths with different concentrations of ionic charge carriers [169]. Because their function depends on the annihilation of charge carriers, these are generally made using acids and bases that react to form water [169]. Zhao et al. devised an enhanced type II diode by using ions that react to form an insoluble precipitate instead of water. When these ions are driven into the junction (under reverse bias), they rapidly form an impermeable salt barrier that prevents further ion migration [170]. Under forward bias, the large fields induced across the precipitate barrier rip it back apart into its constituent ions. The non-interacting counterions to the reactive ions are then free to cross the junction and sustain an ionic current.

Recently, type III diodes have been constructed from aqueous polyelectrolytes. One popular choice is to use PSS and PDAC as the polyanion and polycation respectively, with platinum foil as the electrode [171–173]. Carye et al. and Zhang et al. used these polymers directly while Wang et al. embedded them in a double network. The direct use of the polymers led to a much higher rectification ratio, but limited the device stretchability, while the double network diode retained performance up to a stretch of 4. One disadvantage of these water based systems was that the breakdown voltages were low. At around -2 V, the currents began to increase dramatically as water was dissociated at the junction. Because the electrodes in these devices were made from platinum or silver and thus semipolarizable, the measured response of the

diode was a function of the electrode interface in addition to the polyelectrolyte junction. For example, while the open circuit voltage of the system was likely in the hundreds of mV range [173], the device only conducted well in forward bias above 2 V when the platinum electrodes were able to split water efficiently [168]. Han et al. made a similar type III diode with non-polarizable electrodes and demonstrated a turn on voltage near 0 V [174].

There are two ways researchers have solved this low breakdown voltage. First, water dissociation can be avoided by eliminating water from the system. Kim et al. demonstrated a diode junction made from acrylate polymers swelled with ionic liquids [142]. Second, the water splitting reaction can be suppressed by reducing the local electric field or removing a base catalyst by changing the chemistry [175, 176]. Gabriëlsson et al. demonstrated both suppression approaches. By placing a neutral gel between the polycationic and polyanionic layers of the junction, the junction electric field spreads over a much larger distance and water splitting was eliminated. Unfortunately, it dramatically harms another key diode metric, the switching time. The forward-to-reverse-bias switching time of this neutral layer device is on the order of hundreds of seconds, since all the ions must be extracted from the neutral layer before current stops flowing. By instead replacing the polyammonium group on their polycation with a polyphosphonium, they removed the weak base catalyst that speeds up water dissociation. With this polycation, they were able to reverse bias the junction up to -40 V without water splitting, and still retain the fast (~ 4 s) switching time of direct contact junctions [175].

Gabriëlsson et al. also demonstrated that the neutral gel approach can be improved by changing to a type I diode. By using hydroxide and hydrogen ions as the mobile species, ions do not accumulate in the neutral region during forward bias, and so there is nothing to extract in reverse bias. To create a source of these mobile ions, Gabriëlsson et al. additionally proposed using two other direct contact type I junctions oppositely biased to the main junction to generate mobile hydroxide and hydrogen on the fly [177].

3.3.3 Transistors

Transistors are three terminal devices where the current or voltage at one terminal controls the current between the other two terminals. Transistors are widely used in both digital and analog circuitry as the foundation for logic gates and amplifiers respectively. Ionic transistors would enable a wide variety of ionic circuits. There has been much research into creating transistors with nano-pores and microfluidic channels [178, 179], but relatively little progress in solid state bulk transistors that do not require nano-structuring. As far as the authors are aware, there are only five such transistors documented in the literature; three are Bipolar Junction Transistors (BJTs), while two are Junction Field Effect Transistors (JFETs). One of these JFETs has only been proposed but not experimentally realized.

3.3.3.1 Bipolar Junction Transistors

BJTs consist of two junctions in series with opposite polarity. The three terminals spanning these two junctions are the emitter,

base, and collector (**Figure 6D, Supplementary Video S3**). The ionic version of the BJT is simpler than the semiconductor equivalent in two ways [1]: these transistors do not rely on quantum mechanics or different energy bands to function [2]; the selective mobility in each polymer is created chemically rather than electronically. In a polymer BJT with a polycation base and a polyanion emitter and collector, the ionic current flowing from the emitter to the collector is controlled by the current flowing through the base. This is analogous to a PNP semiconductor BJT. If the materials and currents are reversed, then a device analogous to an NPN transistor is created. BJTs rely on movement of minority carriers for their operation. Key metrics for ionic BJTs are switching time, amplification gain, and side reactions.

For PNP devices, each junction acts like a type III diode. Forward biasing the emitter–base junction ($V_B < V_E$) injects a large number of mobile minority cations into the base. Some of the minority mobile ions that enter the base, flow out of the base terminal, comprising the emitter–base current. The base–collector junction is reverse biased ($V_B > V_C$), such that a large electric field is created across this junction. This field creates a depletion region of majority carriers (anions) in the base at the base–collector junction. The injected minority cations however, feel this field and migrate across the base–collector junction where they become majority carriers again and carry the source–drain current.

Tybrant et al. made a transistor using overoxidized PSS as the CEM and a commercial Fumatech membrane as the AEM with neutral PEG in the middle. PEG decreased the magnitude of the electric field between the polyelectrolyte membranes. This allowed for reverse bias voltages greater than 1.5 V on each of the junctions without water splitting. The junctions were on the order of 25 μm by 200 μm . They achieved a current amplification of about 10, and a switching time on the order of 10s. They used this transistor to deliver neurotransmitter to some cells [180, 181].

Gabrielsson et al. took their polyphosphonium material previously used to create a diode and used it to create a BJT. Their material contains no water, enabling them to remove the neutral gel separator that Tybrant et al. used. Polyphosphonium was patterned over an over-oxidized PEDOT:PSS base. PEDOT:PSS was additionally used as the electrodes. They report a gain of up to 43.9, with a switching time of under 2 s. They attribute this fast switching time to the small (2 μm) distance between collector and emitter and high voltages that are enabled by not having water splitting [182].

Kim et al. created a water-free BJT from an ionic liquid and acrylate polyelectrolytes. These are the same materials they used to create their diode described in **Section 3.3.2**. Their device had a switching time comparable to Gabrielsson et al., but suffered from a low gain of only slightly greater than one.

3.3.3.2 Field Effect Transistors

The second type of ionic transistor being researched is the Field Effect Transistor, which is quite different from the BJT (**Figure 6E, Supplementary Video S4**). By analogy with traditional semiconductors FETs, in an N-channel Junction

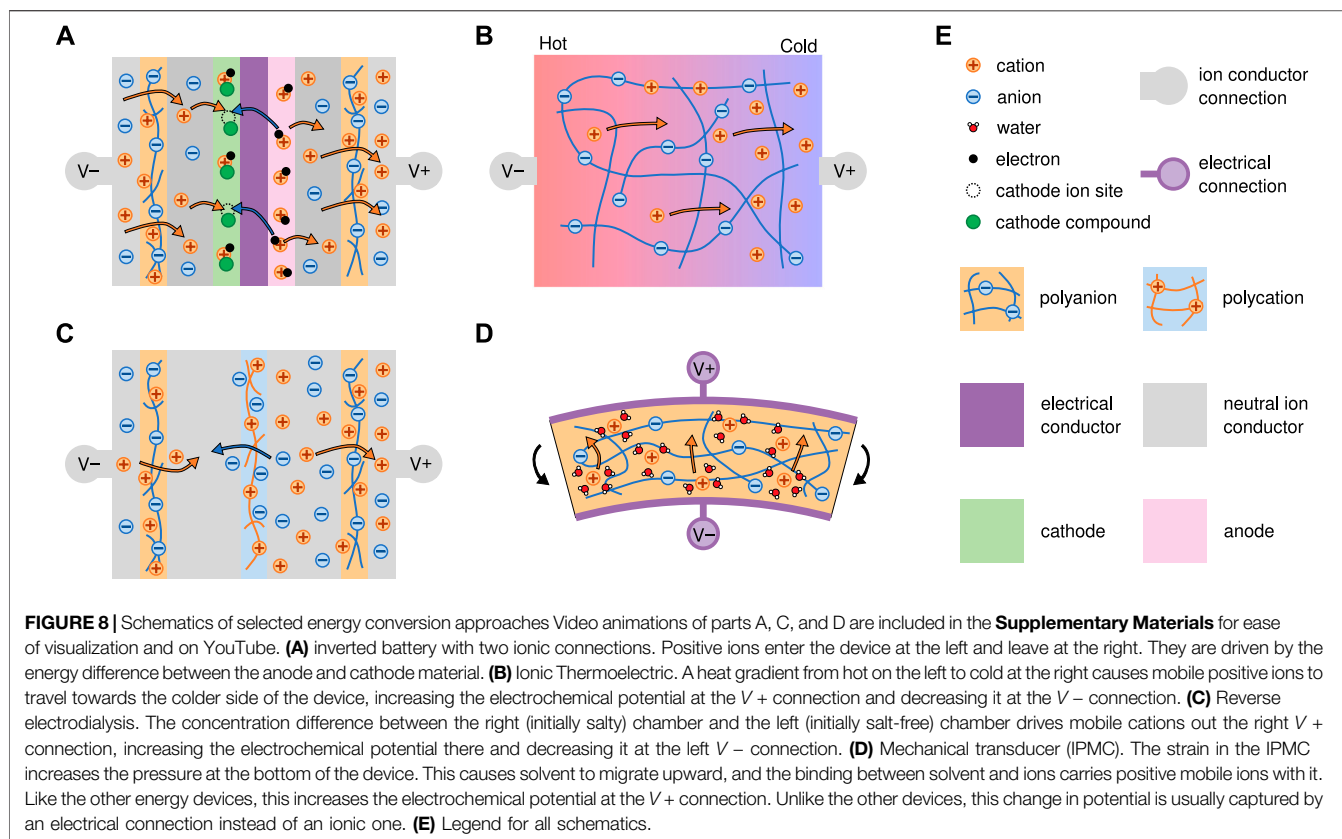
FET (JFET), there would be a continuous polycation connecting the source to the drain terminals. This polycationic channel is then surrounded by a polyanion, which is connected to the gate terminal. When the gate is disconnected or at high voltage, anions can flow freely through the polycationic channel. When the gate is at a low potential, the gate–channel junction is driven into a stronger reverse bias. This bias increases the size of the depletion regions at the edge of the channels by forcing cations out, thereby reducing the current flowing through the device. With sufficient reverse bias, the depletion regions completely close off the channel, stopping the current flowing from source to drain. Boon et al. modeled how a fully ionic P-channel FET might be created [183]. The main challenge in creating ionic FETs is the small size of the depletion regions in ionic junctions due to their high carrier concentration and thus small Debye length. The polycation channel must have a diameter on the order of 10s of nanometers. Boon et al. proposed creating these channels by using an electrically conductive nano-porous carbon matrix. Instead of a continuous polyionic channel, a solvent filled nano-porous membrane would be capped by two polycationic membranes. This means that the junction is formed between a metal and an anion filled channel, rather than a polycation and a polyanion directly, but the operational mechanism is similar. Their model predicts an amplification factor of up to 6, with a switching time of better than 10 ms. They simulated these transistors in three configurations and demonstrated good functionality in all three cases. Zhong et al. [184] made a nanoscale FET using a Maleic–chitosan channel controlled by a silicon gate. Their device controls 2.5 nA of current from source to drain with a gate voltage swing of 30 V.

3.4 Energy Sources

Ionic devices need power sources in order to perform most of their functions. While a myriad of energy sources exist for powering traditional electronic circuits, the natural form of power for ionic devices is in the form of ions. In other words, the devices we have discussed will be run off of concentration gradients and electric fields. In fact, because the mobile species are often charged, concentration gradients lead to electrochemical potential gradients. Thus, in order to power our devices, we need something that is soft, polymeric, and able to set up an electrochemical potential gradient. This section explores four technologies that promise to do so: batteries, reverse-electrodialysis, mechanical harvesters, and thermoelectrics (**Figure 8, Supplementary Videos S5–S7**). The capacitors from **Section 3.3.1** have the potential to be used as energy storage devices, but are included there because of how they are used in existing literature.

3.4.1 Flexible Batteries

In traditional robotics, batteries are a ubiquitous source of power. They also work internally with ions, and so appear naturally adaptable for powering ionic circuits and devices. Wang et al. demonstrated how this might be done in their 2017 paper on inverted batteries [185]. By inverting the construction of a traditional lithium ion battery, the previously internal ion



transport now drives power through an external circuit. This inverted configuration is shown in **Figure 8A** and **Supplementary Video S5**. Electrons flow inside the battery and are compensated by ions flowing through the external terminals. One challenge is that lithium metal used as an anode is incompatible with water. In order to use a water-free battery electrolyte at the same time as a water based external circuitry, they used water impermeable cation exchange membranes near each battery terminal to provide a barrier between the internal and external electrolytes. This concept promises to allow the significant advancements in soft battery technology to relatively directly carry over to ionic circuitry [185].

There are still, however, obstacles to realizing fully soft polymeric batteries. There are two main challenges: creating effective polymer electrolytes and creating flexible, high density electrodes. Approaches to both of these problems can additionally be broken down into two camps. The first approach is to integrate thin films or small particles of conventional electrochemical materials into soft substrates. In this direction (“structural design”), the emphasis is to provide flexibility to materials that already have the desired chemical functionalities but are otherwise inflexible. In a second approach, one can start with soft materials, then impart the desired electrochemical properties (“materials design”). Either approach has led to successful energy conversion and storage devices. However, improving the performance and stability to match those of traditional electrochemical components remains a challenge.

Soft-ionic electrolytes have been extensively studied as gels, polymers, or composites [186–194], promising to replace the existing norms of hard solid-state electrolytes and liquid electrolyte/porous separator combinations. To meet this ambitious goal, soft-ionic electrolytes must fulfill the requirements of solid-state electrolytes, which include high ionic conductivity, mechanical and electrochemical stability, ease of processing, and low interfacial resistance [195]. These are similar to the requirements for good ionic conductors as discussed in **Section 3.1**, but with additional restrictions unique to batteries: electrochemical stability and low interfacial resistance. For example, many battery chemistries like lithium are incompatible with water, and so cannot use the variety of water based polyelectrolytes. Fulfilling these requirements, however, has required trade-offs. For example, the free volume in polymers can benefit the ion’s motion but has a negative effect on the mechanical stability [196, 197]. Similarly, hydrocarbon polymers have low cost, good chemical stability, and easy integration with manufacturing; however, their low dielectric constants restrict the ion-pair dissociation required for high conductivity [195, 198]. Gel-based electrolytes using an inert polymer matrix (polyvinylidene fluoride, “PVdF”) with battery salts (LiPF₆) and solvents (mixture of carbonates) offer high energy density and ease of packaging [199]; however, the limited electrolyte fraction, interaction between ions and polymers, and poor interfacial contacts restrict the conductivity of gel-based battery systems [200, 201].

At present, these electrolyte membranes need to be combined with non-polymeric flexible electrodes to achieve flexible batteries. Because batteries with high gravimetric and volumetric energy densities require dense, well-packed electrodes and electrolytes, structural design and ease of processing are a critical consideration for the soft-ionic-materials integration [202]. This is especially true for electrodes containing inorganic oxides, which must be sufficiently thick to provide reasonable capacity, but not too thick such that the rigidity compromises the device mechanics. In addition to this trade-off, the interface between electrode and current collector must be able to handle bending stress. These challenges highlight the need to understand the electronic and ionic connectivity at the interface within and between electrodes, electrolytes, and current collectors. We point the readers to several excellent reviews on the structural design of flexible electrodes [203–205].

Electrodes are also tackled from a “materials design” approach. One example is to functionalize carbon nanomaterials, which are conductive and intrinsically flexible. The functionalized groups can be molecular or nanoparticles [206–210]. The goal is to increase the energy density and stability to match the performance of conventional batteries. To enable this improvement, one can increase the voltage windows by engineering the electronic structure of the redox center and their density [211–213]. With these advances, carbon-based electrodes with $>1000 \text{ mA h g}^{-1}$ capacities can now be obtained [212, 213]. However, these organic compounds were developed for energy density and thus their mechanical properties have yet to be evaluated. The next steps are to further improve the volumetric energy density and stability of these organic materials, and study more extensive combinations of batteries and ionic devices.

3.4.2 Reverse Electrodialysis

Reverse electrodialysis (RED) is a promising technology that generates electric power from a salinity gradient. In RED, an alternating series of AEMs and CEMs separate compartments of concentrated salt solution and less concentrated solution. These high and low salinity regions can take the form of fluids or gels. Salt wants to flow from high concentration to low concentration, but the specific configuration of ion exchange membranes means that one ion can only flow inside the RED device, while the counterion can only flow through the terminals and external circuit. This constraint on ion paths turns a salt flow into an electrochemical power source. The magnitude of power generated is primarily determined by the salinity gradient and the number of chambers in the RED device [214, 215] (**Figure 8C**, **Supplementary Video S6**). RED devices in literature are often characterized while connected to external electrical circuits with electrodes, but this is not required when using them with other ionic components. RED device performance and membrane stack design has been analyzed using multiphysics models similar to those discussed previously but with additional fluid motion terms (Navier-Stokes) [216–219].

Baek et al. reported using a miniaturized RED patch made from commercial IEMs to power a electro-chemiluminescent bio-sensing

microchip [220]. An eight-layered patch was capable of generating 1.9 V while a ten-layered RED patch produced 2.5 V. The electrode-less RED patch was also used as an ionic power source for active transdermal drug delivery [221]. Shroeder et al. made a RED system that used hydrogels instead of liquid solutions for the salt chamber [222]. The maximum power density per unit cell was 27 mW cm^{-2} while the open-circuit voltage reached up to 110 V by stacking gels in series. It was also demonstrated that power density can be increased by reducing the thickness of hydrogel films to as thin as a few hundred nanometers [223]. Based on these results, exploration into ultrathin membranes with improved permselectivity and conductivity based on advanced materials opens up novel possibilities for robust energy harvesting with RED [224–230].

One challenge with most existing RED systems is that they need a mechanical pump or regular injection of saline solution into every compartment to maintain power levels. This makes traditional RED impractical for stand-alone ionic devices. To overcome this limitation, Baek et al. developed a RED device that uses precipitation and dissolution to maintain the ion concentrations in the high and low salinity chambers [231]. In this device, two different salts are placed into alternating high concentration chambers. These salts are chosen such that they are individually soluble, but both metathesis products are insoluble. Ions entering the low concentration chambers thus precipitate, maintaining that low concentration. The maximum power of a 20-stack precipitation assisted RED was $\sim 100 \mu\text{W}$ while the open circuit potential maintained 90% of the maximum after $\sim 5 \text{ hrs}$. One potential challenge with this approach is the precipitate clogging the ion exchange membranes after extended periods of use.

3.4.3 Mechanical Ion Transducers

Energy harvesting from mechanical motion or vibration is a sustainable power source for various wearable devices and ionic gradient generation. Efforts have been dedicated to several types of mechanical transducers, such as electromagnetics, electrostatics, electrokinetics, piezoelectrics or triboelectrics [232–238]. However, these energy generators are efficient in collecting mechanical/vibrational energy at a relatively high frequency ($>20 \text{ Hz}$) while dramatically compromising their energy harvesting performance with reduced operating frequency ($<1 \text{ Hz}$), where most unused natural mechanical energy or human motion takes place. Ionic transducers can be soft and provide durable energy as well as sensitive in low frequencies, where electricity generation is based on ionic transport and conduction.

We mentioned ionic polymer metal composites (IPMCs) as sensors in **Section 3.1**, but with mechano-electric characteristics, high compliance and wet environment compatibility, they are also frequently applied to energy harvesting in underwater applications. Therefore, IPMCs have been used to harvest energy from base excitation [239], the flutter induced vibration of a heavy flag [240], hydroelastic impact under impulsive loading [241], fluid-induced mechanical buckling [242], hydrodynamic coupling between arrays of IPMC strip [243], fluid-structure interactions from a miniaturized turbine [244], and vibration of a biomimetic tail [245]. The harvested

power ranged from 10^{-2} W to 10^{-9} W for centimeter-scale systems while the performance was heavily determined by the energy exchange between the coherent fluid structure, like vortex rings and pairs, and IPMCs [246]. This is shown in **Figure 8D** and **Supplementary Video S1**.

Other types of mechanical energy harvesters operative in a low frequency regime utilize different materials and mechanisms. Kim et al. [247] utilized electrochemically active materials to realize stress-composition coupling, where lithium ions migrating across an electrolyte membrane (microporous polypropylene monolayer soaked with electrolyte) under a bending-induced pressure difference drive electron flow in the outer circuit. Energy can also be harvested by cyclically changing the surface area and capacitance of ionic interfaces. Harvesting energy from electrode-ionic-conductor interfaces has been demonstrated [248, 249]. By using a polycation-polyanion interface instead, one can take advantage of the rectification behavior of the interface, creating DC currents from AC mechanical inputs [143, 250]. Hou et al. [250] proposed a flexible ionic diode that is an organic p-n junction with asymmetric ionic liquid/ionomer and multi-walled carbon nanotube incorporated into the matrix. The equilibrium of the p-n junction can be disrupted upon mechanical stimuli, producing a power density of $2 \mu\text{Wcm}^{-3}$ at a frequency of 0.1 Hz.

Ionic triboelectric nanogenerators (TENG) harvest energy based on contact electrification and electrostatic induction [251–253]. Pu et al. created a skin-like TENG with PAAm-LiCl hydrogel as ionic conductor, realizing high stretchability and transparency as well as a maximum power density of $3.5 \mu\text{Wcm}^{-2}$ [252]. Hwang et al. developed an ion-pump based TENG (iTENG), where the capacitance of the device changed with increasing number of free ions under pressure [253, 254]. The maximum power density achieved by a single iTENG is 2.2Wcm^{-2} . Although the mechanisms governing ionic TENG are still somewhat debated, they are typically understood and modeled in terms of ion transfer from differential surface affinity of unbound anions and cations, asymmetrical separation of water, and mechanochemical generation of ions and radicals [255–260]. Density functional theory is a particularly powerful approach for computationally investigating these mechanisms. The output performances of ionic TENGs could be further enhanced by maximizing the surface area, therefore maximizing the surface electrostatic charge density through surface treatments and modifications, or by increasing the dielectric permittivity through material optimization combining polymers with graphene sheets, graphite particles, and high-dielectric nanoparticles.

3.4.4 Ionic Thermoelectrics

Thermoelectric (TE) devices generate current from an applied temperature gradient, allowing for the re-conversion of waste heat to usable energy. Fundamental to these devices is the Seebeck effect, where a voltage is generated given a temperature gradient. The maximum efficiency of a TE material is determined by its figure of merit ZT:

$$ZT = \frac{S^2 \sigma}{\kappa} T, \quad (11)$$

where κ is the thermal conductivity in W/mK, S is the Seebeck coefficient in V/K, σ is the electrical conductivity in S/m, and T is the temperature in Kelvin. The Seebeck effect is caused by the thermal diffusion of charge carriers. In traditional TE materials, the charge carriers are electrons or holes. Recently, ionic TE materials have gained interest, in which ions serve as a significant charge carrier. The ionic contribution to the Seebeck coefficient can be quantified via $S_{\text{ionic}} = \frac{F}{\sigma T} z^{(i)} C^{(i)} D_T$, where D_T is the Soret thermal diffusion coefficient of the ions in $\text{m}^2 \text{s}^{-1} \text{K}^{-1}$ [261]. In a conventional ionic TE, the Soret effect [262] creates a voltage on top of the electronic contribution. The large Seebeck coefficients in ionic TEGs could originate from temperature-dependent dissociation of ions [263]. Unlike electrons, ions cannot pass the interface between the TE material and external electrodes. Thus, one way to utilize the Soret effect is via ionic thermoelectric supercapacitors (ITESCs) [264]. These devices could be used, for example, to harness solar energy, in which the ITESC charges via the Sun's heat during the day and discharges at night [265]. ITESCs were also found to generate a voltage from a small temperature difference, making them appealing for wearables and other low-grade heat recovery [266].

To leverage the high conductivity of electrons and high Seebeck coefficient of ions, research has been conducted on mixed ionic and electronic conductors. For example, PEDOT:PSS is known for achieving a high ZT value of 0.42 in the organic TE field [267]. The addition of sodium ions further improved ionic conductivity and Seebeck coefficients [268]. Higher humidity is beneficial because water molecules weaken electrostatic potential traps created by anions [268]. Ionics and electronic conductivities could be simultaneously enhanced by altering oxygen positions on polymer side chains [269]. Additionally, the Seebeck coefficient was improved in various ways, including type II cellulose ionic conductors associated with high Na⁺ selectivity [270], a gelatin matrix modified with added ion providers and redox couple species [271], an ionogel composed of ionic liquids and PVDF-HFP [272], and a low-cost ambipolar ionic polymer gel [273].

Despite recent work, a gap persists with respect to understanding the thermodynamics governing ionic thermodiffusion, making predictions of material performance difficult [265]. Furthermore, it is challenging to operate a purely ionic TEG in continuous mode.

4 DISCUSSION

Ionic devices and components have seen significant progress in the past 10 years. Here we discuss what they can enable and where we see opportunities for improvement.

Ideally, ionic devices should not be limited by a requirement to interface with traditional electronics. Much existing research involves tethering ionic devices to computers and power supplies that provide power and analyze the signals. While this approach is sufficient for characterizing single component performance in the lab, it has two problems in the context of ionic devices: 1) the devices are not tested with the boundary conditions they will experience

when combined, and 2) it restricts the application of the devices to those where external computer connections are possible. As such, more development is needed to develop testing techniques that impose boundary conditions that components would experience within larger ionic circuits.

Some researchers have approached this challenge by using one ionic component to test the performance of another, while others seek to verify that performance in the context of a larger system. In that first category, Han et al combined a reverse electro dialysis energy source with hydrogel wires and a type III polyelectrolyte diode to make a complete circuit. This allowed them to characterize the diode behavior under DC ion current, in contrast with the AC methods popular with electrode boundary conditions [274]. In the second category we have logic gates. They are similar in architecture to traditional semiconductor diode based logic gates. Logic devices of up to three components have been experimentally realized in a few different architectures [171, 174, 177, 275].

Ionic devices are often conceptualized by analogy with traditional semiconductors. While this works well for many designs, there are a couple of key differences between ionic and electronic devices that will only become more relevant as more complicated circuits are created. First there are differences in scale. Ionics have conductivities on par with doped semiconductors, but even the best ionic conductors are many orders of magnitude higher resistance than metal wires (10 vs. 10^6 Sm^{-1}). The carrier concentrations required to reach these modest conductivities result in characteristic length scales for ionics that are much smaller than their semiconductor equivalents. As mentioned in **Section 2.2**, the Debye-Hückel length for these systems is on the order of nano-meters while for semiconductors it is on the order of microns. This places strong limits on the behavior of junction-based devices like JFETs. These differences in scale are supplemented by differences in kind. For example, ionic devices are capable of simultaneously containing multiple charge carriers. This, combined with the fact that most charge carriers used are non-annihilating, means that the design space for ionic devices is both different and broader than traditional semiconductors. This benefit also has consequences for how ionic devices can be combined together. Many devices rely on specific ions in order to function well. This means that many components cannot be directly connected with one another. If that was tried, then the function of the components would change over time as the individual ions mixed together. In general, the long term functioning of a device is jeopardized if the thermodynamic equilibrium of each component is not the same as the operating condition of the device. For example, type I diodes that rely on the mixing of an acid and a base solution are difficult to integrate into a larger device both because they require something to regenerate that acid and base solution, and because the extreme pHs constrain the other connected ionic components.

The field also currently lacks, as far as we are aware, standardized metrics for comparing ionic devices against each other. This leads to a wide variety of device analyses, with little directly comparable performance. Selection of centralized metrics would be aided by more research and analysis of what are currently the critical bottlenecks in performance. These may be significantly different

from those present when the ionic devices are used as part of a larger electronic system. For example, thermoionic power systems and diodes are limited by the interfacial capacitance when connected to electrical conductors [142, 261], but this bottleneck might disappear when they are used in ionic circuits because there is no electrode to saturate.

Further, we need better modelling and design methods if we are to invent more complex ionic circuits. Current approaches rely heavily on finite element solutions to the full continuum equations of state. This works well for individual components, but will likely have trouble scaling to simulate larger circuits that involve of many junctions. Computational approaches in general, while not the focus of this review paper, have proved rather difficult because of the large spread in length and time scales of the various effects at play in an ionic device.

5 CONCLUSION

This review paper discussed the current state and potential of soft ionic materials in the context of stretchable fully ionic devices. Soft ionics are poised to play a key role in a new era of biocompatible medical devices, fully soft robots, and novel signal processing systems. Many of the elements needed for these devices have already been developed—energy converters/harvesters, sensors, actuators, signal transmitters, capacitors, diodes, and transistors—but have not been designed for interacting with other ionic elements. Designing elements with device integration in mind, standardization of performance metrics, and expansion of system level modeling approaches will enable these devices to reach their potential.

AUTHOR CONTRIBUTIONS

MT, NB, and MS contributed to conceptualization. MT, NB, XZ, SK, and MS contributed to visualization. All authors contributed to writing - original draft and writing - review and editing. MS and ZT were responsible for funding acquisition.

FUNDING

The authors acknowledge the support through Defense Advanced Research Project Agency Young Faculty Award (DARPA YFA; HR00112010004). SK and ZT acknowledge the Academic Venture Fund from Cornell Atkinson Center for Sustainability.

SUPPLEMENTARY MATERIAL

The Supplementary Material for this article can be found online at: <https://www.frontiersin.org/articles/10.3389/fphy.2022.890845/full#supplementary-material>

REFERENCES

- Keplinger C, Sun J-Y, Foo CC, Rothmund P, Whitesides GM, Suo Z. Stretchable, Transparent, Ionic Conductors. *Science* (2013) 341:984–7. doi:10.1126/science.1240228
- El-Atab N, Mishra RB, Al-Modaf F, Joharji L, Alsharif AA, Alamoudi H, et al. Soft Actuators for Soft Robotic Applications: A Review. *Adv Intell Syst* (2020) 2:2000128. doi:10.1002/aisy.202000128
- Zhao G, Lv B, Wang H, Yang B, Li Z, Junfang R, et al. Ionogel-based Flexible Stress and Strain Sensors. *Int J Smart Nano Mater* (2021) 12:307–36. doi:10.1080/19475411.2021.1958085
- Flory PJ. *Principles of Polymer Chemistry*. Cornell University Press (1953). Google-Books-ID: CQ0EbEkT5R0C.
- Buenger D, Topuz F, Groll J. Hydrogels in Sensing Applications. *Prog Polym Sci* (2012) 37:1678–719. doi:10.1016/j.progpolymsci.2012.09.001
- Liu X, Liu J, Lin S, Zhao X. Hydrogel Machines. *Mater Today* (2020) 36:102–24. doi:10.1016/j.mattod.2019.12.026
- Chester SA, Anand L. A Coupled Theory of Fluid Permeation and Large Deformations for Elastomeric Materials. *J Mech Phys Sol* (2010) 58:1879–906. doi:10.1016/j.jmps.2010.07.020
- Liu Z, Toh W, Ng TY. Advances in Mechanics of Soft Materials: A Review of Large Deformation Behavior of Hydrogels. *Int J Appl Mech* (2015) 07:1530001. doi:10.1142/S1758825115300011
- Lei J, Li Z, Xu S, Liu Z. Recent Advances of Hydrogel Network Models for Studies on Mechanical Behaviors. *Acta Mech Sin* (2021) 37:367–86. doi:10.1007/s10409-021-01058-2
- Boyce MC. Direct Comparison of the Gent and the Arruda-Boyce Constitutive Models of Rubber Elasticity. *Rubber Chem Tech* (1996) 69:781–5. doi:10.5254/1.3538401
- Wang M, Zhang P, Shamsi M, Thelen JL, Qian W, Truong VK, et al. Tough and Stretchable Ionogels by *In Situ* Phase Separation. *Nat Mater* (2022) 21:359–65. doi:10.1038/s41563-022-01195-4
- Sun J-Y, Zhao X, Illeperuma WRK, Chaudhuri O, Oh KH, Mooney DJ, et al. Highly Stretchable and Tough Hydrogels. *Nature* (2012) 489:133–6. doi:10.1038/nature11409
- Gong JP. Why Are Double Network Hydrogels So Tough? *Soft Matter* (2010) 6:2583–90. doi:10.1039/B924290B
- Liu Y, He W, Zhang Z, Lee B. Recent Developments in Tough Hydrogels for Biomedical Applications. *Gels* (2018) 4:46. doi:10.3390/gels4020046
- Chen Q, Chen H, Zhu L, Zheng J. Engineering of Tough Double Network Hydrogels. *Macromol Chem Phys* (2016) 217:1022–36. doi:10.1002/macp.201600038
- Zhang L, Brostowitz NR, Cavicchi KA, Weiss RA. Perspective: Ionomer Research and Applications. *Macromol React Eng* (2014) 8:81–99. doi:10.1002/mren.201300181
- Sarkar S, SenGupta AK, Prakash P. The Donnan Membrane Principle: Opportunities for Sustainable Engineered Processes and Materials. *Environ Sci Technol* (2010) 44:1161–6. doi:10.1021/es9024029
- Donnan FG. Theory of Membrane Equilibria and Membrane Potentials in the Presence of Non-dialysing Electrolytes. A Contribution to Physical-Chemical Physiology. *J Membr Sci* (1995) 100:45–55. doi:10.1016/0376-7388(94)00297-c
- Duncan AJ, Akle BJ, Long TE, Leo DJ. Ionomer Design for Augmented Charge Transport in Novel Ionic Polymer Transducers. *Smart Mater Struct* (2009) 18:104005. doi:10.1088/0964-1726/18/10/104005
- Hong W, Zhao X, Suo Z. Large Deformation and Electrochemistry of Polyelectrolyte Gels. *J Mech Phys Sol* (2010) 58:558–77. doi:10.1016/j.jmps.2010.01.005
- Wallmersperger T, Kröplin B, Gülch RW. Coupled Chemo-Electro-Mechanical Formulation for Ionic Polymer Gels-Numerical and Experimental Investigations. *Mech Mater* (2004) 36:411–20. doi:10.1016/s0167-6636(03)00068-1
- Suo Z. Theory of Dielectric Elastomers. *Acta Mechanica Solida Sinica* (2010) 23:549–78. doi:10.1016/s0894-9166(11)60004-9
- Henann DL, Chester SA, Bertoldi K. Modeling of Dielectric Elastomers: Design of Actuators and Energy Harvesting Devices. *J Mech Phys Sol* (2013) 61:2047–66. doi:10.1016/j.jmps.2013.05.003
- Basics of Measuring the Dielectric Properties of Materials (Keysight Technologies). *Keysight Application Note 5989-2589* (2020).
- Narayan S, Stewart EM, Anand L. Coupled Electro-Chemo-Elasticity: Application to Modeling the Actuation Response of Ionic Polymer-Metal Composites. *J Mech Phys Sol* (2021) 152:104394. doi:10.1016/j.jmps.2021.104394
- Poghossian A, Abouzar MH, Schöning MJ. Capacitance-voltage and Impedance Characteristics of Field-Effect EIS Sensors Functionalised with Polyelectrolyte Multilayers. *IRBM* (2008) 29:149–54. doi:10.1016/j.irbmet.2007.11.018
- Agmon N. The Grotthuss Mechanism. *Chem Phys Lett* (1995) 244:456–62. doi:10.1016/0009-2614(95)00905-J
- Kreuer K-D. Proton Conductivity: Materials and Applications. *Chem Mater* (1996) 8:610–41. doi:10.1021/cm950192a
- Cukierman S. Et Tu, Grotthuss! and Other Unfinished Stories. *Biochim Biophys Acta (Bba) - Bioenerg* (2006) 1757:876–85. doi:10.1016/j.bbabi.2005.12.001
- Riccardi D, König P, Prat-Resina X, Yu H, Elstner M, Frauenheim T, et al. "Proton Holes" in Long-Range Proton Transfer Reactions in Solution and Enzymes: A Theoretical Analysis. *J Am Chem Soc* (2006) 128:16302–11. doi:10.1021/ja065451j
- Deng Y, Josberger E, Jin J, Roudsari AF, Helms BA, Zhong C, et al. H⁺-type and OH⁻-type Biological Protonic Semiconductors and Complementary Devices. *Sci Rep* (2013) 3:2481. doi:10.1038/srep02481
- Miyake T, Rolandi M. Grotthuss Mechanisms: from Proton Transport in Proton Wires to Bioprotonic Devices. *J Phys Condens Matter* (2016) 28:023001. doi:10.1088/0953-8984/28/2/023001
- Choi P, Jalani NH, Datta R. Thermodynamics and Proton Transport in Nafion. *J Electrochem Soc* (2005) 152:E123. doi:10.1149/1.1859814
- Sanders EH, McGrady KA, Wnek GE, Edmondson CA, Mueller JM, Fontanella JJ, et al. Characterization of Electrospun Nafion Films. *J Power Sourc* (2004) 129:55–61. doi:10.1016/j.jpowsour.2003.11.020
- Ochi S, Kamishima O, Mizusaki J, Kawamura J. Investigation of Proton Diffusion in Nafion117 Membrane by Electrical Conductivity and NMR. *Solid State Ionics* (2009) 180:580–4. doi:10.1016/j.ssi.2008.12.035
- Sone Y, Ekdunge P, Simonsson D. Proton Conductivity of Nafion 117 as Measured by a Four-Electrode AC Impedance Method. *J Electrochem Soc* (1996) 143:1254–9. doi:10.1149/1.1836625
- Berezina NP, Kononenko NA, Dyomina OA, Gnsin NP. Characterization of Ion-Exchange Membrane Materials: Properties vs Structure. *Adv Colloid Interf Sci* (2008) 139:3–28. doi:10.1016/j.cis.2008.01.002
- Long L, Wang S, Xiao M, Meng Y. Polymer Electrolytes for Lithium Polymer Batteries. *J Mater Chem A* (2016) 4:10038–69. doi:10.1039/C6TA02621D
- Iost RM, Crespilho FN. Layer-by-layer Self-Assembly and Electrochemistry: Applications in Biosensing and Bioelectronics. *Biosens Bioelectron* (2012) 31:1–10. doi:10.1016/j.bios.2011.10.040
- Wu J, Yuan XZ, Martin JJ, Wang H, Zhang J, Shen J, et al. A Review of PEM Fuel Cell Durability: Degradation Mechanisms and Mitigation Strategies. *J Power Sourc* (2008) 184:104–19. doi:10.1016/j.jpowsour.2008.06.006
- Inaba M, Kinumoto T, Kiriake M, Umebayashi R, Tasaka A, Ogumi Z. Gas Crossover and Membrane Degradation in Polymer Electrolyte Fuel Cells. *Electrochimica Acta* (2006) 51:5746–53. doi:10.1016/j.electacta.2006.03.008
- Silberstein MN, Boyce MC. Hygro-thermal Mechanical Behavior of Nafion during Constrained Swelling. *J Power Sourc* (2011) 196:3452–60. doi:10.1016/j.jpowsour.2010.11.116
- Farhat TR, Hammond PT. Designing a New Generation of Proton-Exchange Membranes Using Layer-By-Layer Deposition of Polyelectrolytes. *Adv Funct Mater* (2005) 15:945–54. doi:10.1002/adfm.200400318
- Argun AA, Ashcraft JN, Hammond PT. Highly Conductive, Methanol Resistant Polyelectrolyte Multilayers. *Adv Mater* (2008) 20:1539–43. doi:10.1002/adma.200703205
- Liu DS, Ashcraft JN, Mannarino MM, Silberstein MN, Argun AA, Rutledge GC, et al. Spray Layer-By-Layer Electrospun Composite Proton Exchange Membranes. *Adv Funct Mater* (2013) 23:3087–95. doi:10.1002/adfm.201202892
- Ding Y, Zhang J, Chang L, Zhang X, Liu H, Jiang L. Preparation of High-Performance Ionogels with Excellent Transparency, Good Mechanical

- Strength, and High Conductivity. *Adv Mater* (2017) 29:1704253. doi:10.1002/adma.201704253
47. Wu Y, Joseph S, Aluru NR. Effect of Cross-Linking on the Diffusion of Water, Ions, and Small Molecules in Hydrogels. *J Phys Chem B* (2009) 113:3512–20. doi:10.1021/jp808145x
 48. Yang CH, Chen B, Lu JJ, Yang JH, Zhou J, Chen YM, et al. Ionic cable. *Extreme Mech Lett* (2015) 3:59–65. doi:10.1016/j.eml.2015.03.001
 49. Chen B, Lu JJ, Yang CH, Yang JH, Zhou J, Chen YM, et al. Highly Stretchable and Transparent Ionogels as Nonvolatile Conductors for Dielectric Elastomer Transducers. *ACS Appl Mater Inter* (2014) 6:7840–5. doi:10.1021/am501130t
 50. Ming X, Zhang C, Cai J, Zhu H, Zhang Q, Zhu S. Highly Transparent, Stretchable, and Conducting Ionoelastomers Based on Poly(ionic Liquid)s. *ACS Appl Mater Inter* (2021) 13:31102–10. doi:10.1021/acscami.1c05833
 51. Shi L, Jia K, Gao Y, Yang H, Ma Y, Lu S, et al. Highly Stretchable and Transparent Ionic Conductor with Novel Hydrophobicity and Extreme-Temperature Tolerance. *Research* (2020) 2020:1–10. doi:10.34133/2020/2505619
 52. Cao Y, Morrissey TG, Acome E, Allec SI, Wong BM, Keplinger C, et al. A Transparent, Self-Healing, Highly Stretchable Ionic Conductor. *Adv Mater* (2017) 29:1605099. doi:10.1002/adma.201605099
 53. Li Ra., Fan T, Chen G, Zhang K, Su B, Tian J, et al. Autonomous Self-Healing, Antifreezing, and Transparent Conductive Elastomers. *Chem Mater* (2020) 32:874–81. doi:10.1021/acs.chemmater.9b04592
 54. Zhao J, Gong J, Wang G, Zhu K, Ye K, Yan J, et al. A Self-Healing Hydrogel Electrolyte for Flexible Solid-State Supercapacitors. *Chem Eng J* (2020) 401:125456. doi:10.1016/j.cej.2020.125456
 55. Lileg O, Ribbeck K. Biological Hydrogels as Selective Diffusion Barriers. *Trends Cel Biol* (2011) 21:543–51. doi:10.1016/j.tcb.2011.06.002
 56. Cheng C, Yaroshchuk A, Bruening ML. Fundamentals of Selective Ion Transport through Multilayer Polyelectrolyte Membranes. *Langmuir* (2013) 29:1885–92. doi:10.1021/la304574e
 57. Farhat TR, Schlenoff JB. Ion Transport and Equilibria in Polyelectrolyte Multilayers. *Langmuir* (2001) 17:1184–92. doi:10.1021/la001298+
 58. Cheng W, Liu C, Tong T, Epsztein R, Sun M, Verduzco R, et al. Selective Removal of Divalent Cations by Polyelectrolyte Multilayer Nanofiltration Membrane: Role of Polyelectrolyte Charge, Ion Size, and Ionic Strength. *J Membr Sci* (2018) 559:98–106. doi:10.1016/j.memsci.2018.04.052
 59. Femmer R, Mani A, Wessling M. Ion Transport through Electrolyte/polyelectrolyte Multi-Layers. *Sci Rep* (2015) 5:11583. doi:10.1038/srep11583
 60. Dykstra JE, Biesheuvel PM, Bruning H, Ter Heijne A. Theory of Ion Transport with Fast Acid-Base Equilibrations in Bioelectrochemical Systems. *Phys Rev E* (2014) 90:013302. doi:10.1103/PhysRevE.90.013302
 61. Tang Y, Chen C, Ye YS, Xue Z, Zhou X, Xie X. The Enhanced Actuation Response of an Ionic Polymer-Metal Composite Actuator Based on Sulfonated Polyphenylsulfone. *Polym Chem* (2014) 5:6097–107. doi:10.1039/C4PY00663A
 62. Morales D, Palleau E, Dickey MD, Velev OD. Electro-actuated Hydrogel Walkers with Dual Responsive Legs. *Soft Matter* (2014) 10:1337–48. doi:10.1039/C3SM51921J
 63. Jin ML, Park S, Kim J-S, Kwon SH, Zhang S, Yoo MS, et al. An Ultrastable Ionic Chemiresistor Skin with an Intrinsically Stretchable Polymer Electrolyte. *Adv Mater* (2018) 30:1706851. doi:10.1002/adma.201706851
 64. Kim CC, Lee HH, Oh KH, Sun JY. Highly Stretchable, Transparent Ionic Touch Panel. *Science* (2016) 353:682. doi:10.1126/science.aaf8810
 65. Lee H-R, Kim C-C, Sun J-Y. Stretchable Ionics - A Promising Candidate for Upcoming Wearable Devices. *Adv Mater* (2018) 30:1704403. doi:10.1002/adma.201704403
 66. Bar-Cohen Y, Anderson IA. Electroactive Polymer (EAP) Actuators-Background Review. *Mech Soft Mater* (2019) 1:5. doi:10.1007/s42558-019-0005-1
 67. Melling D, Martinez JG, Jager EWH. Conjugated Polymer Actuators and Devices: Progress and Opportunities. *Adv Mater* (2019) 31:1808210. doi:10.1002/adma.201808210
 68. Majidi C. Soft-Matter Engineering for Soft Robotics. *Adv Mater Tech* (2019) 4:1800477. doi:10.1002/admt.201800477
 69. Kim J, Kim JW, Kim HC, Zhai L, Ko H-U, Muthoka RM. Review of Soft Actuator Materials. *Int J Precis Eng Manuf* (2019) 20:2221–41. doi:10.1007/s12541-019-00255-1
 70. Hajiesmaili E, Clarke DR. Dielectric Elastomer Actuators. *J Appl Phys* (2021) 129:151102. doi:10.1063/5.0043959
 71. Guo Y, Liu L, Liu Y, Leng J. Review of Dielectric Elastomer Actuators and Their Applications in Soft Robots. *Adv Intell Syst* (2021) 3:2000282. doi:10.1002/aisy.202000282
 72. Feng C, Hemantha Rajapaksha CP, Jáklí A. Ionic Elastomers for Electric Actuators and Sensors. *Engineering* (2021) 7:581–602. doi:10.1016/j.eng.2021.02.014
 73. Zou M, Li S, Hu X, Leng X, Wang R, Zhou X, et al. Progresses in Tensile, Torsional, and Multifunctional Soft Actuators. *Adv Funct Mater* (2021) 31:2007437. doi:10.1002/adfm.202007437
 74. Kim KJ, Shahinpoor M. Ionic Polymer Metal Composites: II. Manufacturing Techniques. *Smart Mater Struct* (2003) 12:65–79. doi:10.1088/0964-1726/12/1/308
 75. Oguro K. Bending of an Ion-Conducting Polymer Film-Electrode Composite by an Electric Stimulus at Low Voltage. *J Micromachine Soc* (1992) 5:27–30.
 76. Shahinpoor M. Conceptual Design, Kinematics and Dynamics of Swimming Robotic Structures Using Ionic Polymeric Gel Muscles. *Smart Mater Struct* (1992) 1:91–4. doi:10.1088/0964-1726/1/1/014
 77. Sadeghipour K, Salomon R, Neogi S. Development of a Novel Electrochemically Active Membrane and 'smart' Material Based Vibration Sensor/damper. *Smart Mater Struct* (1992) 1:172–9. doi:10.1088/0964-1726/1/2/012
 78. Hao M, Wang Y, Zhu Z, He Q, Zhu D, Luo M. A Compact Review of IPMC as Soft Actuator and Sensor: Current Trends, Challenges, and Potential Solutions from Our Recent Work. *Front Robot AI* (2019) 6:129. doi:10.3389/frobt.2019.00129
 79. MohdIsa W, Hunt A, Hosseinia SH. Sensing and Self-Sensing Actuation Methods for Ionic Polymer-Metal Composite (IPMC): A Review. *Sensors* (2019) 19:3967. doi:10.3390/s19183967
 80. Shahinpoor M, Bar-Cohen Y, Xue T, Harrison JS, Smith JG. *Some Experimental Results on Ionic Polymer-Metal Composites (IPMC) as Biomimetic Sensors and Actuators*. San Diego, CA (1998). p. 251. doi:10.1117/12.316870
 81. Konyo M, Konishi Y, Tadokoro S, Kishima T. *Development of Velocity Sensor Using Ionic Polymer-Metal Composites*. San Diego, CA (2004). p. 307. doi:10.1117/12.540266
 82. Wang J, Wang Y, Zhu Z, Wang J, He Q, Luo M. The Effects of Dimensions on the Deformation Sensing Performance of Ionic Polymer-Metal Composites. *Sensors* (2019) 19:2104. doi:10.3390/s19092104
 83. Nemat-Nasser S, Li JY. Electromechanical Response of Ionic Polymer-Metal Composites. *J Appl Phys* (2000) 87:3321–31. doi:10.1063/1.372343
 84. López-Díaz A, Martín-Pacheco A, Rodríguez AM, Herrero MA, Vázquez AS, Vázquez E. Concentration Gradient-Based Soft Robotics: Hydrogels Out of Water. *Adv Funct Mater* (2020) 30:2004417. doi:10.1002/adfm.202004417
 85. White BT, Long TE. Advances in Polymeric Materials for Electromechanical Devices. *Macromol Rapid Commun* (2019) 40:1800521. doi:10.1002/marc.201800521
 86. Liu X, He B, Wang Z, Tang H, Su T, Wang Q. Tough Nanocomposite Ionogel-Based Actuator Exhibits Robust Performance. *Sci Rep* (2014) 4:6673. doi:10.1038/srep06673
 87. Kim O, Kim SY, Park B, Hwang W, Park MJ. Factors Affecting Electromechanical Properties of Ionic Polymer Actuators Based on Ionic Liquid-Containing Sulfonated Block Copolymers. *Macromolecules* (2014) 47:4357–68. doi:10.1021/ma500869h
 88. Albehajian HA, Piedrahita CR, Cao J, Soliman M, Mitra S, Kyu T. Mechano-electrical Transduction of Polymer Electrolyte Membranes: Effect of Branched Networks. *ACS Appl Mater Inter* (2020) 12:7518–28. doi:10.1021/acscami.9b15599
 89. Piedrahita CR, Yue P, Cao J, Lee H, Rajapaksha CP, Feng C, et al. Flexoelectricity in Flexoionic Polymer Electrolyte Membranes: Effect of Thiosiloxane Modification on Poly(ethylene Glycol) Diacrylate and Ionic Liquid Electrolyte Composites. *ACS Appl Mater Inter* (2020) 12:16978–86. doi:10.1021/acscami.0c2328
 90. Wang Y, Zhu Z, Liu J, Chang L, Chen H. Effects of Surface Roughening of Nafion 117 on the Mechanical and Physicochemical Properties of Ionic Polymer-Metal Composite (IPMC) Actuators. *Smart Mater Struct* (2016) 25:085012. doi:10.1088/0964-1726/25/8/085012

91. He Q, Yu M, Song L, Ding H, Zhang X, Dai Z. Experimental Study and Model Analysis of the Performance of IPMC Membranes with Various Thickness. *J Bionic Eng* (2011) 8:77–85. doi:10.1016/S1672-6529(11)60001-2
92. Kim K, Shahinpoor M. A Novel Method of Manufacturing Three-Dimensional Ionic Polymer-Metal Composites (IPMCs) Biomimetic Sensors, Actuators and Artificial Muscles. *Polymer* (2002) 43:797–802. doi:10.1016/S0032-3861(01)00648-6
93. Bahramzadeh Y, Shahinpoor M. A Review of Ionic Polymeric Soft Actuators and Sensors. *Soft Robotics* (2014) 1:38–52. doi:10.1089/soro.2013.0006
94. Buechler MA, Leo DJ. Characterization and Variational Modeling of Ionic Polymer Transducers. *J Vibration Acoust* (2007) 129:113–20. doi:10.1115/1.2424973
95. Aureli M, Porfiri M. Nonlinear Sensing of Ionic Polymer Metal Composites. *Continuum Mech Thermodyn* (2013) 25:273–310. doi:10.1007/s00161-012-0253-x
96. Nardinocchi P, Pezzulla M, Placidi L. Thermodynamically Based Multiphysics Modeling of Ionic Polymer Metal Composites. *J Intell Mater Syst Structures* (2011) 22:1887–97. doi:10.1177/1045389X11417195
97. Wallmersperger T, Horstmann A, Kroplin B, Leo DJ. Thermodynamical Modeling of the Electromechanical Behavior of Ionic Polymer Metal Composites. *J Intell Mater Syst Structures* (2009) 20:741–50. doi:10.1177/1045389X08096356
98. Nemat-Nasser S. Micromechanics of Actuation of Ionic Polymer-Metal Composites. *J Appl Phys* (2002) 92:2899–915. doi:10.1063/1.1495888
99. Cha Y, Porfiri M. Mechanics and Electrochemistry of Ionic Polymer Metal Composites. *J Mech Phys Sol* (2014) 71:156–78. doi:10.1016/j.jmps.2014.07.006
100. Galante S, Lucantonio A, Nardinocchi P. The Multiplicative Decomposition of the Deformation Gradient in the Multiphysics Modeling of Ionic Polymers. *Int J Non-Linear Mech* (2013) 51:112–20. doi:10.1016/j.jnonlinmec.2013.01.005
101. Newbury KM, Leo DJ. Electromechanical Modeling and Characterization of Ionic Polymer Benders. *J Intell Mater Syst Structures* (2002) 13:51–60. doi:10.1177/1045389X02013001978
102. Newbury KM, Leo DJ. Linear Electromechanical Model of Ionic Polymer Transducers -Part I: Model Development. *J Intell Mater Syst Structures* (2003) 14:333–42. doi:10.1177/1045389X03034976
103. Park K, Lee H-K. Evaluation of Circuit Models for an IPMC (Ionic Polymer-Metal Composite) Sensor Using a Parameter Estimate Method. *J Korean Phys Soc* (2012) 60:821–9. doi:10.3938/jkps.60.821
104. Qaviandam Z, Naghavi N, Safaie J. A New Approach to Improve IPMC Performance for Sensing Dynamic Deflection: Sensor Biasing. *IEEE Sensors J* (2020) 20:8614–22. doi:10.1109/JSEN.2020.2986091
105. Glazer PJ, van Erp M, Embrechts A, Lemay SG, Mendes E. Role of pH Gradients in the Actuation of Electro-Responsive Polyelectrolyte Gels. *Soft Matter* (2012) 8:4421–6. doi:10.1039/C2SM07435D
106. Doi M, Matsumoto M, Hirose Y. Deformation of Ionic Polymer Gels by Electric fields. *Macromolecules* (1992) 25:5504–11. doi:10.1021/ma00046a058
107. Hamlen RP, Kent CE, Shafer SN. Electrolytically Activated Contractile Polymer. *Nature* (1965) 206:1149–50. doi:10.1038/2061149b0
108. Osada Y, Okuzaki H, Hori H. A Polymer Gel with Electrically Driven Motility. *Nature* (1992) 355:242–4. doi:10.1038/355242a0
109. Tanaka T, Nishio I, Sun ST, Ueno-Nishio S. Collapse of Gels in an Electric Field. *Science* (1982) 218:467. doi:10.1126/science.218.4571.467
110. Shiga T, Kurauchi T. Breding of Polyacrylic Acid Gel in Elec-Tnc Fields. *Polym Preprints Jpn* (1985) 34:509.
111. Shiga T. Deformation and Viscoelastic Behavior of Polymer Gels in Electric fields. *Adv Polym Sci* (1997) 134:133. doi:10.1007/3-540-68449-2_2
112. Osada Y, Gong J-P. Soft and Wet Materials: Polymer Gels. *Adv Mater* (1998) 10:827–37. doi:10.1002/(sici)1521-4095(199808)10:11<827::aid-adma827>3.0.co;2-l
113. Kim SJ, Kim HI, Park SJ, Kim IY, Lee SH, Lee TS, et al. Behavior in Electric fields of Smart Hydrogels with Potential Application as Bio-Inspired Actuators. *Smart Mater Struct* (2005) 14:511–4. doi:10.1088/0964-1726/14/4/008
114. Safronov AP, Shakhnovich M, Kalganov A, Kamalov IA, Shklyar TF, Blyakhman FA, et al. DC Electric fields Produce Periodic Bending of Polyelectrolyte Gels. *Polymer* (2011) 52:2430–6. doi:10.1016/j.polymer.2011.03.048
115. Jabbari E, Tavakoli J, Sarvestani AS. Swelling Characteristics of Acrylic Acid Polyelectrolyte Hydrogel in a Dc Electric Field. *Smart Mater Struct* (2007) 16:1614–20. doi:10.1088/0964-1726/16/5/015
116. Jackson N, Stam F. Optimization of Electrical Stimulation Parameters for Electro-Responsive Hydrogels for Biomedical Applications. *J Appl Polym Sci* (2015) 132. doi:10.1002/app.41687
117. Segalman DJ, Witkowski WR, Adolf DB, Shahinpoor M. Theory and Application of Electrically Controlled Polymeric Gels. *Smart Mater Struct* (1992) 1:95–100. doi:10.1088/0964-1726/1/1/015
118. Attaran A, Brummund J, Wallmersperger T. Modeling and Simulation of the Bending Behavior of Electrically-Stimulated Cantilevered Hydrogels. *Smart Mater Struct* (2015) 24:035021. doi:10.1088/0964-1726/24/3/035021
119. Attaran A, Keller K, Wallmersperger T. Modeling and Simulation of Hydrogels for the Application as finger Grippers. *J Intell Mater Syst Structures* (2018) 29:371–87. doi:10.1177/1045389X17708040
120. Leichsenring P, Wallmersperger T. Time-dependent Chemo-Electro-Mechanical Behavior of Hydrogel-Based Structures. In: HE Naguib, editor. *Behavior and Mechanics of Multifunctional Materials and Composites XII*. Denver, United States: SPIE (2018). p. 55. doi:10.1117/12.2297693
121. Migliorini L, Santaniello T, Yan Y, Lenardi C, Milani P. Low-voltage Electrically Driven Homeostatic Hydrogel-Based Actuators for Underwater Soft Robotics. *Sensors Actuators B: Chem* (2016) 228:758–66. doi:10.1016/j.snb.2016.01.110
122. Engel L, Berkh O, Adesanya K, Shklovsky J, Vanderleyden E, Dubrue P, et al. Actuation of a Novel Pluronic-Based Hydrogel: Electromechanical Response and the Role of Applied Current. *Sensors Actuators B: Chem* (2014) 191:650–8. doi:10.1016/j.snb.2013.10.031
123. Liu Q, Dong Z, Ding Z, Hu Z, Yu D, Hu Y, et al. Electroresponsive Homogeneous Polyelectrolyte Complex Hydrogels from Naturally Derived Polysaccharides. *ACS Sust Chem. Eng.* (2018) 6:7052–63. doi:10.1021/acsuschemeng.8b00921
124. Yang S, Liu G, Cheng Y, Zheng Y. Electroresponsive Behavior of Sodium Alginate-G-Poly (Acrylic Acid) Hydrogel under DC Electric Field. *J Macromolecular Sci A* (2009) 46:1078–82. doi:10.1080/10601320903245433
125. Yang S, Liu G, Wang X, Song J. Electroresponsive Behavior of a Sulfonated Poly(vinyl Alcohol) Hydrogel and its Application to Electrodriven Artificial Fish. *J Appl Polym Sci* (2010) 117:2346–53. doi:10.1002/app.32069
126. Yang S, Liu G, Xu F. Electroresponsive Behavior of Sulfonated Benzal Poly(vinyl Alcohol) Hydrogel under Direct-Current Electric Field. *J Macromolecular Sci Part A* (2011) 48:198–203. doi:10.1080/10601325.2011.544629
127. Han D, Farino C, Yang C, Scott T, Browe D, Choi W, et al. Soft Robotic Manipulation and Locomotion with a 3D Printed Electroactive Hydrogel. *ACS Appl Mater Inter* (2018) 10:17512–8. doi:10.1021/acsami.8b04250
128. Cao Z, Liu H, Jiang L. Transparent, Mechanically Robust, and Ultrastable Ionogels Enabled by Hydrogen Bonding between Elastomers and Ionic Liquids. *Mater Horiz* (2020) 7:912–8. doi:10.1039/C9MH01699F
129. Liu S, Li L. Ultrastretchable and Self-Healing Double-Network Hydrogel for 3D Printing and Strain Sensor. *ACS Appl Mater Inter* (2017) 9:26429–37. doi:10.1021/acsami.7b07445
130. Qiao H, Qi P, Zhang X, Wang L, Tan Y, Luan Z, et al. Multiple Weak H-Bonds Lead to Highly Sensitive, Stretchable, Self-Adhesive, and Self-Healing Ionic Sensors. *ACS Appl Mater Inter* (2019) 11:7755–63. doi:10.1021/acsami.8b20380
131. Lai J, Zhou H, Jin Z, Li S, Liu H, Jin X, et al. Highly Stretchable, Fatigue-Resistant, Electrically Conductive, and Temperature-Tolerant Ionogels for High-Performance Flexible Sensors. *ACS Appl Mater Inter* (2019) 11:26412–20. doi:10.1021/acsami.9b10146
132. Wang S, Sun Z, Zhao Y, Zuo L. A Highly Stretchable Hydrogel Sensor for Soft Robot Multi-Modal Perception. *Sensors Actuators A: Phys* (2021) 331:113006. doi:10.1016/j.sna.2021.113006
133. Zhang X, Sheng N, Wang L, Tan Y, Liu C, Xia Y, et al. Supramolecular Nanofibrillar Hydrogels as Highly Stretchable, Elastic and Sensitive Ionic Sensors. *Mater Horiz* (2019) 6:326–33. doi:10.1039/C8MH01188E
134. Yang MJ, Sun HM, Casalbore-Miceli G, Camaioni N, Mari C-M. Poly(propargyl Alcohol) Doped with Sulfuric Acid, a New Proton Conductor Usable for Humidity Sensor Construction. *Synth Met* (1996) 81:65–9. doi:10.1016/0379-6779(96)80230-x

135. Park S-H, Park J-S, Lee C-W, Gong M-S. Humidity Sensor Using Gel Polyelectrolyte Prepared from Mutually Reactive Copolymers. *Sensors Actuators B: Chem* (2002) 86:68–74. doi:10.1016/S0925-4005(02)00149-1
136. Lee C, Joo S, Gong M. Polymeric Humidity Sensor Using Polyelectrolytes Derived from Alkoxysilane Cross-Linker. *Sensors Actuators B: Chem* (2005) 105:150–8. doi:10.1016/S0925-4005(04)00397-1
137. Lv X, Li Y, Li P, Yang M. A Resistive-type Humidity Sensor Based on Crosslinked Polyelectrolyte Prepared by UV Irradiation. *Sensors Actuators B: Chem* (2009) 135:581–6. doi:10.1016/j.snb.2008.10.008
138. Nie H, Schauer NS, Self JL, Tabassum T, Oh S, Geng Z, et al. Light-Switchable and Self-Healable Polymer Electrolytes Based on Dynamic Diarylethene and Metal-Ion Coordination. *J Am Chem Soc* (2021) 143:1562–9. doi:10.1021/jacs.0c11894
139. Gil-González N, Benito-Lopez F, Castaño E, Morant-Miñana MC. Imidazole-based Ionogel as Room Temperature Benzene and Formaldehyde Sensor. *Microchim Acta* (2020) 187:638. doi:10.1007/s00604-020-04625-9
140. Jiang N, Chang X, Hu D, Chen L, Wang Y, Chen J, et al. Flexible, Transparent, and Antibacterial Ionogels toward Highly Sensitive Strain and Temperature Sensors. *Chem Eng J* (2021) 424:130418. doi:10.1016/j.cej.2021.130418
141. Sun J-Y, Keplinger C, Whitesides GM, Suo Z. Ionic Skin. *Adv Mater* (2014) 26:7608–14. doi:10.1002/adma.201403441
142. Kim HJ, Chen B, Suo Z, Hayward RC. Ionoelastomer Junctions between Polymer Networks of Fixed Anions and Cations. *Science* (2020) 367:773–6. doi:10.1126/science.aay8467
143. Sarwar MS, Dobashi Y, Preston C, Wyss JKM, Mirabbasi S, Madden JDW. Bend, Stretch, and Touch: Locating a finger on an Actively Deformed Transparent Sensor Array. *Sci Adv* (2017) 3. doi:10.1126/sciadv.1602200
144. Lei Z, Wang Q, Sun S, Zhu W, Wu P. A Bioinspired Mineral Hydrogel as a Self-Healable, Mechanically Adaptable Ionic Skin for Highly Sensitive Pressure Sensing. *Adv Mater* (2017) 29:1700321. doi:10.1002/adma.201700321
145. He B, Zhou Y, Wang Z, Wang Q, Shen R, Wu S. A Multi-Layered Touch-Pressure Sensing Ionogel Material Suitable for Sensing Integrated Actuators of Soft Robots. *Sensors Actuators A: Phys* (2018) 272:341–8. doi:10.1016/j.sna.2018.01.035
146. Shen Z, Zhu X, Majidi C, Gu G. Cutaneous Ionogel Mechanoreceptors for Soft Machines, Physiological Sensing, and Amputee Prostheses. *Adv Mater* (2021) 33:2102069. doi:10.1002/adma.202102069
147. Esmaeli E, Ganjian M, Rastegar H, Kolahdouz M, Kolahdouz Z, Zhang GQ. Humidity Sensor Based on the Ionic Polymer Metal Composite. *Sensors Actuators B: Chem* (2017) 247:498–504. doi:10.1016/j.snb.2017.03.018
148. Wang Y, Tang G, Zhao C, Wang K, Wang J, Ru J, et al. Experimental Investigation on the Physical Parameters of Ionic Polymer Metal Composites Sensors for Humidity Perception. *Sensors Actuators B: Chem* (2021) 345:130421. doi:10.1016/j.snb.2021.130421
149. Lei H, Lim C, Tan X. Humidity-dependence of IPMC Sensing Dynamics: Characterization and Modeling from a Physical Perspective. *Meccanica* (2015) 50:2663–73. doi:10.1007/s11012-015-0164-6
150. Wang Y, Jia K, Zhang S, Kim HJ, Bai Y, Hayward RC, et al. Temperature Sensing Using Junctions between mobile Ions and mobile Electrons. *Proc Natl Acad Sci* (2022) 119:e2117962119. doi:10.1073/pnas.2117962119
151. Jonsson A, Song Z, Nilsson D, Meyerson BA, Simon DT, Linderöth B, et al. Therapy Using Implanted Organic Bioelectronics. *Sci Adv* (2015) 1. doi:10.1126/sciadv.1500039
152. Sjöström TA, Jonsson A, Gabrielsson EO, Berggren M, Simon DT, Tybrandt K. Miniaturized Ionic Polarization Diodes for Neurotransmitter Release at Synaptic Speeds. *Adv Mater Technol* (2020) 5:1900750. doi:10.1002/admt.201900750
153. Gabrielsson EO, Janson P, Tybrandt K, Simon DT, Berggren M. A Four-Diode Full-Wave Ionic Current Rectifier Based on Bipolar Membranes: Overcoming the Limit of Electrode Capacity. *Adv Mater* (2014) 26:5143–7. doi:10.1002/adma.201401258
154. Larsson KC, Kjäll P, Richter-Dahlfors A. Organic Bioelectronics for Electronic-To-Chemical Translation in Modulation of Neuronal Signaling and Machine-To-Brain Interfacing. *Biochim Biophys Acta (Bba) - Gen Subjects* (2013) 1830:4334–44. doi:10.1016/j.bbagen.2012.11.024
155. Isaksson J, Kjäll P, Nilsson D, Robinson N, Berggren M, Richter-Dahlfors A. Electronic Control of Ca²⁺ Signalling in Neuronal Cells Using an Organic Electronic Ion Pump. *Nat Mater* (2007) 6:673–9. doi:10.1038/nmat1963
156. Yuk H, Lu B, Zhao X. Hydrogel Bioelectronics. *Chem Soc Rev* (2019) 48:1642–67. doi:10.1039/c8cs00595h
157. Carli S, Di Lauro M, Bianchi M, Murgia M, De Salvo A, Prato M, et al. Water-Based PEDOT:Nafion Dispersion for Organic Bioelectronics. *ACS Appl Mater Inter* (2020) 12:29807–17. doi:10.1021/acsami.0c06538
158. Vreeland RF, Atcherley CW, Russell WS, Xie JY, Lu D, Laude ND, et al. Biocompatible PEDOT:Nafion Composite Electrode Coatings for Selective Detection of Neurotransmitters *In Vivo*. *Anal Chem* (2015) 87:2600–7. doi:10.1021/ac502165f
159. Najem JS, Taylor GJ, Weiss RJ, Hasan MS, Rose G, Schuman CD, et al. Memristive Ion Channel-Doped Biomembranes as Synaptic Mimics. *ACS Nano* (2018) 12:4702–11. doi:10.1021/acsnano.8b01282
160. Zhang P, Xia M, Zhuge F, Zhou Y, Wang Z, Dong B, et al. Nanochannel-Based Transport in an Interfacial Memristor Can Emulate the Analog Weight Modulation of Synapses. *Nano Lett* (2019) 19:4279–86. doi:10.1021/acs.nanolett.9b00525
161. Liao K, Lei P, Tu M, Luo S, Jiang T, Jie W, et al. Memristor Based on Inorganic and Organic Two-Dimensional Materials: Mechanisms, Performance, and Synaptic Applications. *ACS Appl Mater Inter* (2021) 13:32606–23. doi:10.1021/acsami.1c07665
162. Koo H-J, So J-H, Dickey MD, Velev OD. Towards All-Soft Matter Circuits: Prototypes of Quasi-Liquid Devices with Memristor Characteristics. *Adv Mater* (2011) 23:3559–64. doi:10.1002/adma.201101257
163. Kim SJ, Kim S, Jang HW. Competing Memristors for Brain-Inspired Computing. *iScience* (2021) 24:101889. doi:10.1016/j.isci.2020.101889
164. Li C, Xiong T, Yu P, Fei J, Mao L. Synaptic Iontronic Devices for Brain-Mimicking Functions: Fundamentals and Applications. *ACS Appl Bio Mater* (2021) 4:71–84. doi:10.1021/acsabm.0c00806
165. Janson P, Gabrielsson EO, Lee KJ, Berggren M, Simon DT. An Ionic Capacitor for Integrated Iontronic Circuits. *Adv Mater Technol* (2019) 4:1800494. doi:10.1002/admt.201800494
166. Martin ST, Akbari A, Chakraborty Banerjee P, Neild A, Majumder M. The Inside-Out Supercapacitor: Induced Charge Storage in Reduced Graphene Oxide. *Phys Chem Chem Phys* (2016) 18:32185–91. doi:10.1039/C6CP06463A
167. Yamamoto T, Doi M. Electrochemical Mechanism of Ion Current Rectification of Polyelectrolyte Gel Diodes. *Nat Commun* (2014) 5:4162. doi:10.1038/ncomms5162
168. Nyamayo K, Triandafilidi V, Keyvani P, Rottler J, Mehrkhodavandi P, Hatzikiakos SG. The Rectification Mechanism in Polyelectrolyte Gel Diodes. *Phys Fluids* (2021) 33:032010. doi:10.1063/1.50040838
169. Iván K, Simon PL, Wittmann M, Noszticzus Z. Electrolyte Diodes with Weak Acids and Bases. I. Theory and an Approximate Analytical Solution. *J Chem Phys* (2005) 123:164509. doi:10.1063/1.2085047
170. Zhao R, He G, Deng Y. Non-water Ionic Diode Based on Bias-dependent Precipitation. *Electrochemistry Commun* (2012) 23:106–9. doi:10.1016/j.elecom.2012.07.019
171. Wang Y, Wang Z, Su Z, Cai S. Stretchable and Transparent Ionic Diode and Logic gates. *Extreme Mech Lett* (2019) 28:81–6. doi:10.1016/j.eml.2019.03.001
172. Cayre OJ, Chang ST, Velev OD. Polyelectrolyte Diode: Nonlinear Current Response of a junction between Aqueous Ionic Gels. *J Am Chem Soc* (2007) 129:10801–6. doi:10.1021/ja072449z
173. Zhang Y, Jeong CK, Wang J, Chen X, Choi KH, Chen LQ, et al. Hydrogel Ionic Diodes toward Harvesting Ultralow-Frequency Mechanical Energy. *Adv Mater* (2021) 33:2103056. doi:10.1002/adma.202103056
174. Han J-H, Kim KB, Kim HC, Chung TD. Ionic Circuits Based on Polyelectrolyte Diodes on a Microchip. *Angew Chem Int Ed* (2009) 48:3830–3. doi:10.1002/anie.200900045
175. Gabrielsson EO, Berggren M. Polyphosphonium-based Bipolar Membranes for Rectification of Ionic Currents. *Biomicrofluidics* (2013) 7:064117. doi:10.1063/1.4850795
176. Simons R. The Origin and Elimination of Water Splitting in Ion Exchange Membranes during Water Demineralisation by Electrodialysis. *Desalination* (1979) 28:41–2. doi:10.1016/S0011-9164(00)88125-4
177. Gabrielsson EO, Tybrandt K, Berggren M. Ion Diode Logics for pH Control. *Lab Chip* (2012) 12:2507–13. doi:10.1039/C2LC40093F
178. Lucas RA, Lin C-Y, Baker LA, Siwy ZS. Ionic Amplifying Circuits Inspired by Electronics and Biology. *Nat Commun* (2020) 11:1568. doi:10.1038/s41467-020-15398-3
179. Sun G, Senapati S, Chang H-C. High-flux Ionic Diodes, Ionic Transistors and Ionic Amplifiers Based on External Ion Concentration Polarization by an Ion

- Exchange Membrane: a New Scalable Ionic Circuit Platform. *Lab Chip* (2016) 16:1171–7. doi:10.1039/C6LC00026F
180. Tybrandt K, Larsson KC, Richter-Dahlfors A, Berggren M. Ion Bipolar Junction Transistors. *Proc Natl Acad Sci U.S.A.* (2010) 107:9929–32. doi:10.1073/pnas.0913911107
 181. Tybrandt K, Gabrielson EO, Berggren M. Toward Complementary Ionic Circuits: The Npn Ion Bipolar Junction Transistor. *J Am Chem Soc* (2011) 133:10141–5. doi:10.1021/ja200492c
 182. Gabrielson EO, Tybrandt K, Berggren M. Polyphosphonium-based Ion Bipolar Junction Transistors. *Biomicrofluidics* (2014) 8:064116. doi:10.1063/1.4902909
 183. Boon N, Olvera de la Cruz M. 'Soft' Amplifier Circuits Based on Field-Effect Ionic Transistors. *Soft Matter* (2015) 11:4793–8. doi:10.1039/C5SM00573F
 184. Zhong C, Deng Y, Roudsari A, Kapetanovic A, Anantram MP, Rolandi M A Polysaccharide Bioprotic Field-Effect Transistor. *Nat Commun* (2011) 2:476. doi:10.1038/ncomms1489
 185. Wang C, Fu K, Dai J, Lacey SD, Yao Y, Pastel G, et al. Inverted Battery Design as Ion Generator for Interfacing with Biosystems. *Nat Commun* (2017) 8:15609. doi:10.1038/ncomms15609
 186. Chen J, Henderson WA, Pan H, Perdue BR, Cao R, Hu JZ, et al. Improving Lithium-Sulfur Battery Performance under Lean Electrolyte through Nanoscale Confinement in Soft Swellable Gels. *Nano Lett* (2017) 17:3061–7. doi:10.1021/acs.nanolett.7b00417
 187. Fan W, Zhang X, Li C, Zhao S, Wang J. UV-initiated Soft-Tough Multifunctional Gel Polymer Electrolyte Achieves Stable-Cycling Li-Metal Battery. *ACS Appl Energy Mater.* (2019) 2:4513–20. doi:10.1021/acs.aem.9b00766
 188. Li Q, Ardebili H. Flexible Thin-Film Battery Based on Solid-like Ionic Liquid-Polymer Electrolyte. *J Power Sourc* (2016) 303:17–21. doi:10.1016/j.jpowsour.2015.10.099
 189. Saunier J, Alloin F, Sanchez JY, Caillon G. Thin and Flexible Lithium-Ion Batteries: Investigation of Polymer Electrolytes. *J Power Sourc* (2003) 119:121:454–9. doi:10.1016/S0378-7753(03)00197-6
 190. Wan J, Xie J, Kong X, Liu Z, Liu K, Shi F, et al. Ultrathin, Flexible, Solid Polymer Composite Electrolyte Enabled with Aligned Nanoporous Host for Lithium Batteries. *Nat Nanotechnol* (2019) 14:705–11. doi:10.1038/s41565-019-0465-3
 191. Gorecki W, Jeannin M, Belorizky E, Roux C, Armand M. Physical Properties of Solid Polymer Electrolyte PEO(LiTFSI) Complexes. *J Phys Condens Matter* (1995) 7:6823–32. doi:10.1088/0953-8984/7/34/007
 192. Kim J-K, Lim YJ, Kim H, Cho G-B, Kim Y. A Hybrid Solid Electrolyte for Flexible Solid-State Sodium Batteries. *Energy Environ. Sci.* (2015) 8:3589–96. doi:10.1039/C5EE01941A
 193. Xie D, Zhang M, Wu Y, Xiang L, Tang Y. A Flexible Dual-Ion Battery Based on Sodium-Ion Quasi-Solid-State Electrolyte with Long Cycling Life. *Adv Funct Mater* (2020) 30:1906770. doi:10.1002/adfm.201906770
 194. Chen L, Li Y, Li S-P, Fan L-Z, Nan C-W, Goodenough JB. PEO/garnet Composite Electrolytes for Solid-State Lithium Batteries: From "Ceramic-In-Polymer" to "Polymer-In-Ceramic". *Nano Energy* (2018) 46:176–84. doi:10.1016/j.nanoen.2017.12.037
 195. Zhao Q, Stalin S, Zhao C-Z, Archer LA. Designing Solid-State Electrolytes for Safe, Energy-Dense Batteries. *Nat Rev Mater* (2020) 5:229–52. doi:10.1038/s41578-019-0165-5
 196. Fan L-Z, Hu Y-S, Bhattacharyya AJ, Maier J. Succinonitrile as a Versatile Additive for Polymer Electrolytes. *Adv Funct Mater* (2007) 17:2800–7. doi:10.1002/adfm.200601070
 197. Lu Y, Cai Y, Zhang Q, Liu L, Niu Z, Chen J. A Compatible Anode/succinonitrile-Based Electrolyte Interface in All-Solid-State Na-CO₂ Batteries. *Chem Sci* (2019) 10:4306–12. doi:10.1039/C8SC05178J
 198. Xu K. Electrolytes and Interphases in Li-Ion Batteries and beyond. *Chem Rev* (2014) 114:11503–618. doi:10.1021/cr500003w
 199. Boudin F, Andrieu X, Jehoulet C, Olsen II. Microporous PVdF Gel for Lithium-Ion Batteries. *J Power Sourc* (1999) 81-82:804–7. doi:10.1016/S0378-7753(99)00154-8
 200. Saikia D, Kumar A. Ionic Conduction in P(VDF-HFP)/PVDF-(PC + DEC)-LiClO₄ Polymer Gel Electrolytes. *Electrochimica Acta* (2004) 49:2581–9. doi:10.1016/j.electacta.2004.01.029
 201. Cheng X, Pan J, Zhao Y, Liao M, Peng H. Gel Polymer Electrolytes for Electrochemical Energy Storage. *Adv Energy Mater.* (2018) 8:1702184. doi:10.1002/aenm.201702184
 202. Chang J, Huang Q, Zheng Z. A Figure of Merit for Flexible Batteries. *Joule* (2020) 4:1346–9. doi:10.1016/j.joule.2020.05.015
 203. Qian G, Liao X, Zhu Y, Pan F, Chen X, Yang Y. Designing Flexible Lithium-Ion Batteries by Structural Engineering. *ACS Energy Lett.* (2019) 4:690–701. doi:10.1021/acsenergylett.8b02496
 204. Zhou G, Li F, Cheng H-M. Progress in Flexible Lithium Batteries and Future Prospects. *Energy Environ. Sci.* (2014) 7:1307–38. doi:10.1039/C3EE43182G
 205. Fu KK, Cheng J, Li T, Hu L. Flexible Batteries: From Mechanics to Devices. *ACS Energy Lett.* (2016) 1:1065–79. doi:10.1021/acsenergylett.6b00401
 206. Li Q, Li D, Wang H, Wang H-g., Li Y, Si Z, et al. Conjugated Carbonyl Polymer-Based Flexible Cathode for Superior Lithium-Organic Batteries. *ACS Appl Mater Inter* (2019) 11:28801–8. doi:10.1021/acsami.9b06437
 207. Zhou M, Li W, Gu T, Wang K, Cheng S, Jiang K. A Sulfonated Polyaniline with High Density and High Rate Na-Storage Performances as a Flexible Organic Cathode for Sodium Ion Batteries. *Chem Commun* (2015) 51:14354–6. doi:10.1039/C5CC05654C
 208. Lee SW, Yabuuchi N, Gallant BM, Chen S, Kim B-S, Hammond PT, et al. High-power Lithium Batteries from Functionalized Carbon-Nanotube Electrodes. *Nat Nanotech* (2010) 5:531–7. doi:10.1038/nnano.2010.116
 209. Wu H, Shevlin SA, Meng Q, Guo W, Meng Y, Lu K, et al. Flexible and Binder-free Organic Cathode for High-Performance Lithium-Ion Batteries. *Adv Mater* (2014) 26:3338–43. doi:10.1002/adma.201305452
 210. Chen H, Armand M, Demailly G, Dolhem F, Poizot P, Tarascon J-M. From Biomass to a Renewable LiXC₆O₆ Organic Electrode for Sustainable Li-Ion Batteries. *ChemSusChem* (2008) 1:348–55. doi:10.1002/cssc.200700161
 211. Wu X, Jin S, Zhang Z, Jiang L, Mu L, Hu Y-S, et al. Unraveling the Storage Mechanism in Organic Carbonyl Electrodes for Sodium-Ion Batteries. *Sci Adv* (2015) 1:e1500330. doi:10.1126/sciadv.1500330
 212. Peng C, Ning G-H, Su J, Zhong G, Tang W, Tian B, et al. Reversible Multi-Electron Redox Chemistry of π -conjugated N-Containing Heteroaromatic Molecule-Based Organic Cathodes. *Nat Energy* (2017) 2:17074. doi:10.1038/energy.2017.74
 213. Lei Z, Yang Q, Xu Y, Guo S, Sun W, Liu H, et al. Boosting Lithium Storage in Covalent Organic Framework via Activation of 14-electron Redox Chemistry. *Nat Commun* (2018) 9:576. doi:10.1038/s41467-018-02889-7
 214. Lacey RE. Energy by Reverse Electrodialysis. *Ocean Eng* (1980) 7:1–47. doi:10.1016/0029-8018(80)90030-X
 215. Campione A, Gurreri L, Ciofalo M, Micale G, Tamburini A, Cipollina A. Electrodialysis for Water Desalination: A Critical Assessment of Recent Developments on Process Fundamentals, Models and Applications. *Desalination* (2018) 434:121–60. doi:10.1016/j.desal.2017.12.044
 216. Tedesco M, Hamelers HVM, Biesheuvel PM. Nernst-Planck Transport Theory for (Reverse) Electrodialysis: I. Effect of Co-ion Transport through the Membranes. *J Membr Sci* (2016) 510:370–81. doi:10.1016/j.memsci.2016.03.012
 217. Gurreri L, Battaglia G, Tamburini A, Cipollina A, Micale G, Ciofalo M. Multi-physical Modelling of Reverse Electrodialysis. *Desalination* (2017) 423:52–64. doi:10.1016/j.desal.2017.09.006
 218. Moya AA. A Nernst-Planck Analysis on the Contributions of the Ionic Transport in Permeable Ion-Exchange Membranes to the Open Circuit Voltage and the Membrane Resistance in Reverse Electrodialysis Stacks. *Electrochimica Acta* (2017) 238:134–41. doi:10.1016/j.electacta.2017.04.022
 219. Jin D, Xi R, Xu S, Wang P, Wu X. Numerical Simulation of Salinity Gradient Power Generation Using Reverse Electrodialysis. *Desalination* (2021) 512:115132. doi:10.1016/j.desal.2021.115132
 220. Baek S, Kwon S-R, Yeon SY, Yoon S-H, Kang CM, Han SH, et al. Miniaturized Reverse Electrodialysis-Powered Biosensor Using Electrochemiluminescence on Bipolar Electrode. *Anal Chem* (2018) 90:4749–55. doi:10.1021/acs.analchem.7b05425
 221. Kwon S-R, Nam SH, Park CY, Baek S, Jang J, Che X, et al. Electrodeless Reverse Electrodialysis Patches as an Ionic Power Source for Active Transdermal Drug Delivery. *Adv Funct Mater* (2018) 28:1705952. doi:10.1002/adfm.201705952
 222. Schroeder TBH, Guha A, Lamoureux A, VanRenterghem G, Sept D, Shtein M, et al. An Electric-Eel-Inspired Soft Power Source from Stacked Hydrogels. *Nature* (2017) 552:214–8. doi:10.1038/nature24670
 223. Ide T, Takeuchi Y, Yanagida T. Development of an Experimental Apparatus for Simultaneous Observation of Optical and Electrical Signals from Single Ion Channels. *Single Mol* (2002) 3:33–42. doi:10.1002/1438-5171(200204)3:1<33::aid-simo33>3.0.co;2-u

224. Sint K, Wang B, Král P. Selective Ion Passage through Functionalized Graphene Nanopores. *J Am Chem Soc* (2008) 130:16448–9. doi:10.1021/ja804409f
225. Siria A, Poncharal P, Bianco A-L, Fulcrand R, Blase X, Purcell ST, et al. Giant Osmotic Energy Conversion Measured in a Single Transmembrane boron Nitride Nanotube. *Nature* (2013) 494:455–8. doi:10.1038/nature11876
226. Angelova P, Vieker H, Weber N-E, Matei D, Reimer O, Meier I, et al. A Universal Scheme to Convert Aromatic Molecular Monolayers into Functional Carbon Nanomembranes. *ACS Nano* (2013) 7:6489–97. doi:10.1021/nn402652f
227. Feng J, Graf M, Liu K, Ovchinnikov D, Dumcenco D, Heiranian M, et al. Single-layer MoS₂ Nanopores as Nanopower Generators. *Nature* (2016) 536:197–200. doi:10.1038/nature18593
228. Moreno C, Vilas-Varela M, Kretz B, Garcia-Lekue A, Costache MV, Paradinas M, et al. Bottom-up Synthesis of Multifunctional Nanoporous Graphene. *Science* (2018) 360:199–203. doi:10.1126/science.aar2009
229. Yang Y, Yang X, Liang L, Gao Y, Cheng H, Li X, et al. Large-area Graphene-Nanomech/carbon-Nanotube Hybrid Membranes for Ionic and Molecular Nanofiltration. *Science* (2019) 364:1057–62. doi:10.1126/science.aau5321
230. Liu X, He M, Calvani D, Qi H, Gupta KBSS, de Groot HJM, et al. Power Generation by Reverse Electrodialysis in a Single-Layer Nanoporous Membrane Made from Core-Rim Polycyclic Aromatic Hydrocarbons. *Nat Nanotechnol* (2020) 15:307–12. doi:10.1038/s41565-020-0641-5
231. Yeon SY, Yun J, Yoon S-h., Lee D, Jang W, Han SH, et al. A Miniaturized Solid Salt Reverse Electrodialysis Battery: a Durable and Fully Ionic Power Source. *Chem Sci* (2018) 9:8071–6. doi:10.1039/C8SC02954G
232. Maamer B, Boughamoura A, Fath El-Bab AMR, Francis LA, Tounsi F. A Review on Design Improvements and Techniques for Mechanical Energy Harvesting Using Piezoelectric and Electromagnetic Schemes. *Energy Convers Manag* (2019) 199:111973. doi:10.1016/j.enconman.2019.111973
233. Wei C, Jing X. A Comprehensive Review on Vibration Energy Harvesting: Modelling and Realization. *Renew Sust Energy Rev* (2017) 74:1–18. doi:10.1016/j.rser.2017.01.073
234. Vidal JV, Slabov V, Kholkin AL, dos Santos MPS. Hybrid Triboelectric-Electromagnetic Nanogenerators for Mechanical Energy Harvesting: A Review. *Nano-micro Lett* (2021) 13:199. doi:10.1007/s40820-021-00713-4
235. Safaei M, Sodano HA, Anton SR. A Review of Energy Harvesting Using Piezoelectric Materials: State-Of-The-Art a Decade Later (2008–2018). *Smart Mater Struct* (2019) 28:113001. doi:10.1088/1361-665X/ab36e4
236. Zou H-X, Zhao L-C, Gao Q-H, Zuo L, Liu F-R, Tan T, et al. Mechanical Modulations for Enhancing Energy Harvesting: Principles, Methods and Applications. *Appl Energy* (2019) 255:113871. doi:10.1016/j.apenergy.2019.113871
237. Gao Q, Cheng T, Wang ZL. Triboelectric Mechanical Sensors-Progress and Prospects. *Extreme Mech Lett* (2021) 42:101100. doi:10.1016/j.eml.2020.101100
238. Fan FR, Tang W, Wang ZL. Flexible Nanogenerators for Energy Harvesting and Self-Powered Electronics. *Adv Mater* (2016) 28:4283–305. doi:10.1002/adma.201504299
239. Aureli M, Prince C, Porfiri M, Peterson SD. Energy Harvesting from Base Excitation of Ionic Polymer Metal Composites in Fluid Environments. *Smart Mater Struct* (2009) 19:015003. doi:10.1088/0964-1726/19/1/015003
240. Giacomello A, Porfiri M. Underwater Energy Harvesting from a Heavy Flag Hosting Ionic Polymer Metal Composites. *J Appl Phys* (2011) 109:084903. doi:10.1063/1.3569738
241. Cha Y, Phan CN, Porfiri M. Energy Exchange during Slamming Impact of an Ionic Polymer Metal Composite. *Appl Phys Lett* (2012) 101:094103. doi:10.1063/1.4748577
242. Cellini F, Cha Y, Porfiri M. Energy Harvesting from Fluid-Induced Buckling of Ionic Polymer Metal Composites. *J Intell Mater Syst Structures* (2014) 25:1496–510. doi:10.1177/1045389X13508333
243. Cellini F, Intartaglia C, Soria L, Porfiri M. Effect of Hydrodynamic Interaction on Energy Harvesting in Arrays of Ionic Polymer Metal Composites Vibrating in a Viscous Fluid. *Smart Mater Struct* (2014) 23:045015. doi:10.1088/0964-1726/23/4/045015
244. Cellini F, Pounds J, Peterson SD, Porfiri M. Underwater Energy Harvesting from a Turbine Hosting Ionic Polymer Metal Composites. *Smart Mater Struct* (2014) 23:085023. doi:10.1088/0964-1726/23/8/085023
245. Cha Y, Verotti M, Walcott H, Peterson SD, Porfiri M. Energy Harvesting from the Tail Beating of a Carangiform Swimmer Using Ionic Polymer-Metal Composites. *Bioinspir Biomim* (2013) 8:036003. doi:10.1088/1748-3182/8/3/036003
246. Peterson SD, Porfiri M. Chapter 14. Energy Exchange between Coherent Fluid Structures and Ionic Polymer Metal Composites, toward Flow Sensing and Energy Harvesting. In: *Ionic Polymer Metal Composites (IPMCs)*. Cambridge, United Kingdom: RSC (2015). p. 1–18. doi:10.1039/9781782627234-00001
247. Kim S, Choi SJ, Zhao K, Yang H, Gobbi G, Zhang S, et al. Electrochemically Driven Mechanical Energy Harvesting. *Nat Commun* (2016) 7:10146. doi:10.1038/ncomms10146
248. Moon JK, Jeong J, Lee D, Pak HK. Electrical Power Generation by Mechanically Modulating Electrical Double Layers. *Nat Commun* (2013) 4:1487. doi:10.1038/ncomms2485
249. Vallem V, Roosa E, Ledin T, Jung W, Kim Ti., Rashid-Nadimi S, et al. A Soft Variable-Area Electrical-Double-Layer Energy Harvester. *Adv Mater* (2021) 33:2103142. doi:10.1002/adma.202103142
250. Hou Y, Zhou Y, Yang L, Li Q, Zhang Y, Zhu L, et al. Flexible Ionic Diodes for Low-Frequency Mechanical Energy Harvesting. *Adv Energy Mater.* (2017) 7:1601983. doi:10.1002/aenm.201601983
251. Parida K, Kumar V, Jiangxin W, Bhavanasi V, Bendi R, Lee PS. Highly Transparent, Stretchable, and Self-Healing Ionic-Skin Triboelectric Nanogenerators for Energy Harvesting and Touch Applications. *Adv Mater* (2017) 29:1702181. doi:10.1002/adma.201702181
252. Pu X, Liu M, Chen X, Sun J, Du C, Zhang Y, et al. Ultrastretchable, Transparent Triboelectric Nanogenerator as Electronic Skin for Biomechanical Energy Harvesting and Tactile Sensing. *Sci Adv* (2017) 9:1700015. doi:10.1126/sciadv.1700015
253. Hwang HJ, Kim JS, Kim W, Park H, Bhatia D, Jee E, et al. An Ultra-Mechanosensitive Visco-Poroelastic Polymer Ion Pump for Continuous Self-Powering Kinematic Triboelectric Nanogenerators. *Adv Energy Mater.* (2019) 9:1803786. doi:10.1002/aenm.201803786
254. Jin ML, Park S, Lee Y, Lee JH, Chung J, Kim JS, et al. An Ultrasensitive, Visco-Poroelastic Artificial Mechanotransducer Skin Inspired by Piezo2 Protein in Mammalian Merkel Cells. *Adv Mater* (2017) 29:1605973. doi:10.1002/adma.201605973
255. McCarty LS, Whitesides GM. Electrostatic Charging Due to Separation of Ions at Interfaces: Contact Electrification of Ionic Electrets. *Angew Chem Int Ed* (2008) 47:2188–207. doi:10.1002/anie.200701812
256. Kim W-G, Kim D-W, Tcho I-W, Kim J-K, Kim M-S, Choi Y-K. Triboelectric Nanogenerator: Structure, Mechanism, and Applications. *ACS Nano* (2021) 15:258–87. doi:10.1021/acsnano.0c09803
257. Pence S, Novotny VJ, Diaz AF. Effect of Surface Moisture on Contact Charge of Polymers Containing Ions. *Langmuir* (1994) 10:592–6. doi:10.1021/la00014a042
258. Diaz AF, Felix-Navarro RM. A Semi-quantitative Tribo-Electric Series for Polymeric Materials: the Influence of Chemical Structure and Properties. *J Electrostatics* (2004) 62:277–90. doi:10.1016/j.elstat.2004.05.005
259. Baytekin HT, Baytekin B, Soh S, Grzybowski BA. Is Water Necessary for Contact Electrification? *Angew Chem* (2011) 123:6898–902. doi:10.1002/ange.201008051
260. Pan S, Zhang Z. Fundamental Theories and Basic Principles of Triboelectric Effect: A Review. *Friction* (2019) 7:2–17. doi:10.1007/s40544-018-0217-7
261. Yang B, Portale G. Ionic Thermoelectric Materials for Waste Heat Harvesting. *Colloid Polym Sci* (2021) 299:465–79. doi:10.1007/s00396-020-04792-4
262. Zhao D, Würger A, Crispin X. Ionic Thermoelectric Materials and Devices. *J Energy Chem* (2021) 61:88–103. doi:10.1016/j.jechem.2021.02.022
263. Kim SL, Hsu J-H, Yu C. Thermoelectric Effects in Solid-State Polyelectrolytes. *Org Elect* (2018) 54:231–6. doi:10.1016/j.orgel.2017.12.021
264. Wang H, Zhao D, Khan ZU, Puzinas S, Jonsson MP, Berggren M, et al. Ionic Thermoelectric Figure of Merit for Charging of Supercapacitors. *Adv Electron Mater* (2017) 3:1700013. doi:10.1002/aenm.201700013
265. Zhao D, Wang H, Khan ZU, Chen JC, Gabrielsson R, Jonsson MP, et al. Ionic Thermoelectric Supercapacitors. *Energy Environ. Sci.* (2016) 9:1450–7. doi:10.1039/C6EE00121A
266. Kim SL, Lin HT, Yu C. Thermally Chargeable Solid-State Supercapacitor. *Adv Energy Mater.* (2016) 6:1600546. doi:10.1002/aenm.201600546

267. Kim G-H, Shao L, Zhang K, Pipe KP. Engineered Doping of Organic Semiconductors for Enhanced Thermoelectric Efficiency. *Nat Mater* (2013) 12:719–23. doi:10.1038/nmat3635
268. Wang H, Ail U, Gabriellsson R, Berggren M, Crispin X. Ionic Seebeck Effect in Conducting Polymers. *Adv Energ Mater.* (2015) 5:1500044. doi:10.1002/aenm.201500044
269. Onorato JW, Wang Z, Sun Y, Nowak C, Flagg LQ, Li R, et al. Side Chain Engineering Control of Mixed Conduction in Oligoethylene Glycol-Substituted Polythiophenes. *J Mater Chem A* (2021) 9:21410–23. doi:10.1039/d1ta05379e
270. Li T, Zhang X, Lacey SD, Mi R, Zhao X, Jiang F, et al. Cellulose Ionic Conductors with High Differential thermal Voltage for Low-Grade Heat Harvesting. *Nat Mater* (2019) 18:608–13. doi:10.1038/s41563-019-0315-6
271. Han C-G, Qian X, Li Q, Deng B, Zhu Y, Han Z, et al. Giant Thermopower of Ionic Gelatin Near Room Temperature. *Science* (2020) 368:1091–8. doi:10.1126/science.aaz5045
272. Cheng H, He X, Fan Z, Ouyang J. Flexible Quasi-Solid State Ionogels with Remarkable Seebeck Coefficient and High Thermoelectric Properties. *Adv Energ Mater.* (2019) 9:1901085. doi:10.1002/aenm.201901085
273. Zhao D, Martinelli A, Willfahrt A, Fischer T, Bernin D, Khan ZU, et al. Polymer Gels with Tunable Ionic Seebeck Coefficient for Ultra-sensitive Printed Thermopiles. *Nat Commun* (2019) 10:1093. doi:10.1038/s41467-019-08930-7
274. Han SH, Kwon S-R, Baek S, Chung T-D. Ionic Circuits Powered by Reverse Electrolysis for an Ultimate Iontronic System. *Sci Rep* (2017) 7:14068. doi:10.1038/s41598-017-14390-0
275. Tybrandt K, Forchheimer R, Berggren M. Logic gates Based on Ion Transistors. *Nat Commun* (2012) 3:871. doi:10.1038/ncomms1869

Conflict of Interest: The authors declare that the research was conducted in the absence of any commercial or financial relationships that could be construed as a potential conflict of interest.

Publisher's Note: All claims expressed in this article are solely those of the authors and do not necessarily represent those of their affiliated organizations, or those of the publisher, the editors and the reviewers. Any product that may be evaluated in this article, or claim that may be made by its manufacturer, is not guaranteed or endorsed by the publisher.

Copyright © 2022 Tepermeister, Bosnjak, Dai, Zhang, Kielar, Wang, Tian, Suntivich and Silberstein. This is an open-access article distributed under the terms of the Creative Commons Attribution License (CC BY). The use, distribution or reproduction in other forums is permitted, provided the original author(s) and the copyright owner(s) are credited and that the original publication in this journal is cited, in accordance with accepted academic practice. No use, distribution or reproduction is permitted which does not comply with these terms.